

# 1     **Adsorptive remediation of environmental pollutants using magnetic** 2                   **hybrid materials as platform adsorbents**

3  
4     Nisar Ali<sup>1\*</sup>, MD Mahamuudul Hasan Riead<sup>1</sup>, Muhammad Bilal<sup>2\*</sup>, Yong Yang<sup>1</sup>, Adnan  
5             Khan<sup>3</sup>, Farman Ali<sup>4</sup>, Shafiul Karim<sup>1</sup>, Cao Zhou<sup>1</sup>, Ye Wenjie<sup>1</sup>, Farooq Sher<sup>5</sup>,  
6                                   Hafiz M.N. Iqbal<sup>6\*</sup>

7  
8     <sup>1</sup>Key Laboratory of Regional Resource Exploitation and Medicinal Research, Faculty of  
9     Chemical Engineering, Huaiyin Institute of Technology, Huaian, Jiangsu Province, P. R.  
10    China.

11    <sup>2</sup>School of Life Science and Food Engineering, Huaiyin Institute of Technology, Huaian  
12    223003, China.

13    <sup>3</sup>Institute of Chemical Sciences, University of Peshawar, Khyber Pakhtunkhwa, 25120  
14    Pakistan.

15    <sup>4</sup>Department of Chemistry, Hazara University, KPK, Mansehra 21300, Pakistan.

16    <sup>5</sup>Department of Engineering, School of Science and Technology, Nottingham Trent  
17    University, Nottingham NG11 8NS, UK.

18    <sup>6</sup>Tecnologico de Monterrey, School of Engineering and Science, Monterrey, 64849,  
19    Mexico.

20    \*Corresponding authors E-mail addresses: nisarali@hyit.edu.cn (N. Ali);  
21    bilaluaf@hotmail.com (M. Bilal); hafiz.iqbal@tec.mx (H.M.N. Iqbal).

## 22 23    **Abstract**

24    Effective separation and remediation of environmentally hazardous pollutants are burning  
25    areas of research because of a constant increase in environmental pollution problems.  
26    An extensive number of emerging contaminants in the environmental matrices result in  
27    serious health consequences in animals, humans, and plants, even at trace levels.  
28    Therefore, it is of paramount significance to quantify these undesirable pollutants, even  
29    at a very low concentration, from the natural environment. Magnetic solid-phase  
30    extraction (MSPE) has recently achieved huge attention because of its strong magnetic  
31    domain and easy separation through an external magnetic field compared with simple

32 solid-phase extraction. Therefore, MSPE appeared the most promising technique for  
33 removing and pre-concentration of emerging pollutants at trace level. Compared to the  
34 normal solid-phase extraction, MSPE as magnetic hybrid adsorbents offers the unique  
35 advantages of distinct nanomaterials and magnetic hybrid materials. It can exhibit efficient  
36 dispersion and rapid recycling when applying to a very complex matrix. This review  
37 highlights the possible environmental applications of magnetic hybrid nanoscale materials  
38 as effective MSPE sorbents to remediate a diverse range of environmentally toxic  
39 pollutants. We believe this study tends to evoke a variety of research thrust that may lead  
40 to novel remediation approaches in the forthcoming years.

41 **Keywords:** Environmental pollutants; Magnetic solid-phase extraction; Adsorbents;  
42 Carbon nanotubes; Metal-organic frameworks; Magnetic hybrid materials

43

## 44 **1. Introduction**

45 The effective separation and removal of toxic pollutants are among the hot research  
46 topics because of the constant increase in ecological inconsistency and environmental  
47 pollution in recent years (Khan et al., 2020; Ali et al., 2020a; Zeb et al., 2020). The  
48 environmental matrices are full of some typical pollutants and can be very harmful to both  
49 land and aquatic life. Some of the emerging contaminants are pesticides, polychlorinated  
50 biphenyls (PCBs), heavy metals, polycyclic aromatic hydrocarbons (PAHs), phthalate  
51 esters (PAEs), bisphenol A (BPA), perfluorinated compounds (PFCs), organic phosphate  
52 flame retardants (OFRs), and so on (Ali et al., 2018; Ahmad et al., 2021; Clarke et al.,  
53 2011). Therefore, even at a low concentration level, it is important to quantify and  
54 determine these destructive pollutants from various sources. In addition, sample  
55 pretreatment procedures need enhanced proficiency and selectivity because of the  
56 complicacy and diversity of the sample matrices (Aziz et al., 2020; Khan et al., 2021a). It  
57 is imperative to design and construct some new adsorbents with high extraction  
58 efficiency, such as amberlite resins, silica gel, graphene oxide, chelating resin, carbon  
59 nanotubes, activated carbon, graphene and so on (Arabi et al., 2017; Bagheri et al., 2019;  
60 Ma et al., 2018; Azzouz et al., 2018).

61 Generally, the most effective and simple technique is dispersive-SPE (DSPE). Followed  
62 by the elution process, in which the reversible interactions between adsorbent and target

63 in a suitable column through adsorption are the base of the following technique (Ötles et  
64 al., 2016; Khan et al., 2021b). A key concern for DSPE is selecting the right adsorbents  
65 such as silica bonded to C18 and frequently used HLB-based hybrid materials. However,  
66 the traditional SPE can be hampered because of the clogging of the adsorbent, the  
67 necessity of toxic solvent in excess during extraction, and high column pressure (Khan et  
68 al., 2019). Carbon dots (C-dots), a new addition to the carbon family, have been widely  
69 reported for many applications. A large number of novel materials can be fabricated using  
70 C-dots as a starting material, such as synthetic, biological, and natural sources of carbon.  
71 A set of desired features like inertness, biocompatibility, easy to functionalization, low  
72 toxicity, and the property of photoluminescence render C-dots preferable for different  
73 applications, such as imaging, drug delivery and biosensing (Wang et al., 2016).  
74 Therefore, a new class of DSPE called MSPE uses magnetic materials as an effective  
75 adsorbent to differentiate and targeted compounds in environmental samples (Ali et al.,  
76 2019).

77 Shortly, the process of solid-phase extraction can be carried out while using MSPE by  
78 diffusing an adsorbent that is magnetic in the specimen sample to enable the adsorption  
79 process of the desired analyte (Ali et al., 2015a; Zhang et al., 2016a). An external magnet  
80 is used to separate the magnetic adsorbent material, which contains the analyte from the  
81 targeted sample matrix after the adsorption process is performed (Scheme 1). The  
82 desired analyte is further desorbed from the MSPEs sorbent and then dissolved in some  
83 suitable desorption solvent after the elution process. For later determination, the  
84 desorption solution can be collected, which is enriched with the target analyte. After that,  
85 the recycling process of the magnetic adsorbent is held. Traditional SPE requires more  
86 time, and the whole filtration and centrifuging processes are very slow, which can be  
87 avoided in MSPE. MSPE shows some promising advantages such as quick separation,  
88 better recycling of sorbent, convenient operation with high extraction efficiency (Fig. 1).

89 A key factor for accomplishing better extraction performance is to select some good  
90 magnetic adsorbents. The addition of magnetic domain imports significantly influences  
91 the anti-interference capability, selectivity, extraction efficiency, and enrichment factor  
92 (Zhang et al., 2016a; Ali et al., 2015b). Various types of magnetism can be exhibited by  
93 magnetic materials such as diamagnetism, ferromagnetism, antiferromagnetism,

94 paramagnetism, and ferrimagnetism. Magnetic materials that show paramagnetism or  
95 ferromagnetism are mainly employed as magnetic cores to construct MSPE adsorbents.  
96 Magnetic nanoparticles are generally made from Ni, Fe, Co and the metal oxides of these  
97 metals, which normally exhibits strong magnetic properties, i.e., ferromagnetism, e.g.,  
98 magnetite ( $\text{Fe}_3\text{O}_4$ ) (Ali et al., 2015c), maghemite, and  $\text{CoFe}_2\text{O}_4$  (Yang et al., 2021a; Ali et  
99 al., 2020b; Zhang et al., 2013). The methods preparing MNPs consist of coprecipitation  
100 synthesis, hydrothermal synthesis, sol-gel synthesis, and solvothermal synthesis. When  
101 the MNPs are used as adsorbents, the magnetic cores agglomerate prepared by the  
102 above methods resulting in a reduction in their magnetic properties. An appropriate  
103 method was needed to fabricate the magnetic core with some functionalized materials is  
104 needed to overcome this limitation (Khan et al., 2021c). Due to their structure and  
105 peculiarities, porous and carbonaceous materials are the most widely used coating  
106 materials. These increase the surface area with abundant active reacting sites and  
107 maintain the oxidation state, followed by improving the stability of MNPs. In addition,  
108 silicon nanomaterials, metallic nanomaterials, chitosan (Ali et al., 2020c,d; Aziz et al.,  
109 2020; Khan et al., 2021d; Yang et al., 2021b), ionic liquids (ILs), and surfactants (Ali et  
110 al., 2020a) are the main MSPE sorbents materials. The mode of interaction between  
111 MSPE sorbent and the target analytes is due to the electrostatic attraction, hydrophobic  
112 force, van der Waals forces, hydrogen bonding, and metal ionic coordination (Zaman et  
113 al., 2019). However, the adsorbent may be interfered with by a complicated matrix due to  
114 these non-selective interactions. Therefore, a beneficial method is the MNPs with  
115 cautiously designed materials known as molecularly imprinted polymers (MIPs) (Zhang  
116 et al., 2015; Nawaz et al., 2020; Ali et al., 2015d). In the last few years, few reviews  
117 published addressing the preparation, properties, and applications of MSPE sorbent  
118 materials. Also, there is lacking some fruitful publications to effectively reviewed the  
119 applications of MSPE sorbents for the enhanced removal of environmental pollutants.  
120 Therefore, in this current work, we tried to sum up the latest available literature in the  
121 advance's magnetic hybrid material as MPSE sorbents and their applications for the  
122 efficient remediation of environmental pollutants.

## 123 **2. Carbon-based magnetic materials as adsorbents**

124 Various carbon-based materials are frequently reported, such as graphitic carbon nitride  
125 (g-C<sub>3</sub>N<sub>4</sub>) carbon nanotubes (CNTs), carbon nanofibers (CNFs), graphene (G) and  
126 graphene oxide (GO), reduced graphene oxide (RGO), carbon-based quantum dots, etc.  
127 (Speltini et al., 2016; Azzouz et al., 2018). Most own superior features, including better  
128 mechanical, chemical, and thermal stability, large surface area, and active sites. To use  
129 these carbons based MSPE sorbent material for the effective removal of environmental  
130 pollutants from complex wastewater matrices. This is possible because MSPE sorbent  
131 gives high specificity and selectivity with reduced medium interference. In this article, we  
132 discussed two main types of magnetic carbonaceous materials as MSPE sorbents. Table  
133 1 explains some of the carbon-based magnetic materials as adsorbents.

### 134 **2.1. Graphene-based composites**

135 Graphene is a well-known carbon-based material that comprises sp<sup>2</sup> hybridized carbon  
136 atoms in a single-atom-thick with a two-dimensional (2-D) structure and hexagonal  
137 structural arrangement in the form of lattice (Hu et al., 2018; Shen et al., 2015). Graphene  
138 gives good applications in extracting organic compounds with a benzene ring with a π-π  
139 stacking in their structure. In the structure of graphene, there are delocalized π-electrons  
140 and a large surface area (Ersan et al., 2017). However, the recycling of graphene from  
141 the sample solutions is challenging because of its hydrophobicity and low weight. If a  
142 polar pollutant contains hydrophilic chemical groups (Lim et al., 2018), Graphene is  
143 ineffective for its absorption (Huang et al., 2018). Hence, to get some practical  
144 applications and meet the specific requirements, proper modification is needed. The  
145 chemical oxidation of graphene leads to graphene oxide (GO), which contains some more  
146 functional groups such as phenolic hydroxyl (-OH), carboxyl (-COOH), epoxy groups (-C-  
147 O-C-). These functional groups can further be modified by fabrication which may show  
148 more affinity for targeted analytes based on the presence of active sites of interaction.  
149 Chemical reduction method used for the preparation of reduced graphene oxides (RGO)  
150 nanosheets. Compared to graphene oxides (GO) RGO contains very few vacancy defects  
151 and oxygen-containing functional groups (He et al., 2016). Incorporating the magnetic  
152 domain to GO and RGO leads to form a very stable magnetic composite MGO and MrGO,  
153 which can be easily recovered and separated from the targeted sample solution and  
154 prevent the loss of MGO sorbent material during the MSPE process.

155 There are many methods for fabricating magnetic graphene oxides composite materials,  
156 such as in-situ coprecipitation, solvothermal, and hydrothermal (Sherlala et al., 2018;  
157 Lingamdinne et al., 2019). Yang et al. used the solvothermal method for the fabrication  
158 of G-doped magnetic nanoparticles to form ( $\text{Fe}_3\text{O}_4/\text{G}$ ) composite material and then  
159 checked the prepared material for the effective removal of 4-bromodiphenyl ether  
160 (BDPE), tetrabromobisphenol A (TBBPA), 2,4,6-tribromophenol (TBP), and 4,4'-  
161 dibromodiphenyl ether (DBDPE) (Yang et al., 2015). Graphene component provides an  
162 extensive system of  $\pi$ -electron. Therefore, the limitations of the simple graphene oxides  
163 (GO) can be reduced by the applications of magnetic content, which can give quick  
164 isolation and separation from the reaction mixture and give more space for the targeted  
165 aromatic compounds by  $\pi$ - $\pi$  stacking and hydrophobic interactions.  $\text{Fe}_3\text{O}_4/\text{G}$  shows 59.9  
166  $\text{emu gL}^{-1}$  of maximum saturation magnetization ( $M_s$ ) value, which proved good  
167 superparamagnetism. Also, the LOD limits of detection are low in the range of 0.2-0.5  $\mu\text{g}$   
168  $\text{L}^{-1}$ , and good recovery rate of about 85.0-105.0% after coupling with high-performance  
169 liquid chromatography-ultraviolet detector (HPLC-UV) to check BFRs in wastewater  
170 samples of water were gained. Without modification, pure magnetic graphene-based  
171 materials usually fail to provide adequate extraction performance because of lean  
172 applications with insufficient adsorption properties for complex and diverse environmental  
173 pollutants. Hence, if Graphene-based materials are further functionalized, they can  
174 considerably help to improve the target analytes selectivity and reduce the interference  
175 from the sample matrices.

176 As graphene oxide is an excellent carbon-based hybrid material containing organic and  
177 inorganic parts and a large surface area with thermal and mechanical stability.  
178 Furthermore, the applications of magnetic graphene oxide are very much promising for  
179 both graphene oxides and magnetic components. An ultrafast, direct, non-toxic, and  
180 green was used to prepare magnetic graphene hybrid materials ( $\text{GO}-\text{Fe}_3\text{O}_4$ ) (Liu et al.,  
181 2018a). Compared to other conventional synthetic methods, this reaction is a very simple  
182 and one step without any production of dangerous pollutants during the whole synthetic  
183 process. Also, the preparation of  $\text{Fe}_3\text{O}_4@\text{GO}$  magnetic hybrid material was confirmed  
184 through the characterization using different instrumental techniques. Furthermore, the  
185 prepared  $\text{Fe}_3\text{O}_4@\text{GO}$  was successfully checked for the adsorption of Methylene blue,

186 and the material show effective adsorption within 30 min. Therefore, Fe<sub>3</sub>O<sub>4</sub>@GO  
187 demonstrates potential applications as an environmental adsorbent.

188 Organophosphorus pesticides (OPPs) detection in water samples, a graphene-based  
189 tetraethoxysilane-methyltrimethoxylane magnetic composite (Fe<sub>3</sub>O<sub>4</sub>@G-TEOS-MTMOS)  
190 was fabricated by Nodeh et al. (2017) as an MSPE adsorbent. The synthetic process  
191 included using the sol-gel method to modify graphene nanosheets and Fe<sub>3</sub>O<sub>4</sub>  
192 nanoparticles, followed by their coating using silica-based porous material. These  
193 functional ingredients of the Fe<sub>3</sub>O<sub>4</sub>@G-TEOS-MTMOS adsorbents exhibit selective  
194 adsorption sites and can be used to effectively adsorption of polar OPPs (phosphamidon,  
195 dimeyhoate) via hydrogen-bonding and non-polar OPPs (diazinon, chlorphyrifos) via π-π  
196 stacking. The adsorption capacity of the Fe<sub>3</sub>O<sub>4</sub>@G-TEOS-MTMOS adsorbents is very  
197 high of about 37.18-76.34 mg g<sup>-1</sup> for both TEOS-MTMOS or Fe<sub>3</sub>O<sub>4</sub>@G or their composites  
198 (Fig. 2). Li et al. (2017a) successfully prepared a magnetic polyethyleneimine-  
199 functionalized RGO-based (Fe<sub>3</sub>O<sub>4</sub>@PEI-RGO) nanohybrid material for the quick  
200 adsorption of MSPE to increase the concentration of the sample with acidic herbicides in  
201 food materials. The RGO component of the modified material import a large surface area  
202 for the exchange of anions can give a large surface area for anion and make the exchange  
203 of PEI, a positively charged polymer. Therefore, the as-synthesized Fe<sub>3</sub>O<sub>4</sub>@PEI-RGO  
204 nanocomposite shows the maximum adsorption of five different herbicides (chiefly  
205 through π-π stacking electrostatic attraction) as compared to Fe<sub>3</sub>O<sub>4</sub>/RGO, Fe<sub>3</sub>O<sub>4</sub>@PEI-  
206 GO, and Fe<sub>3</sub>O<sub>4</sub>@PEI under optimized extraction conditions (Fig. 3).

207 Magnetic graphene oxide Fe<sub>3</sub>O<sub>4</sub>/GO hybrid material was prepared through self-assembly  
208 method and checked their solid phase remediation of polyaromatic hydrocarbons (PAH)  
209 while using different environmental samples (Han et al., 2012). The super hydrophilic  
210 nature of graphene oxides mixed with the charged surface of iron oxide and form a hybrid  
211 material in solution under the electrostatic interaction. Also, different amounts of iron  
212 oxide were also used to effectively control the change in the initial precursor particles.  
213 The structure and surface morphology of the prepared material confirmed through  
214 different characterization techniques such as XRD, VSM, TEM, and XPS, etc. To check  
215 the application of Fe<sub>3</sub>O<sub>4</sub>/GO, five samples of PAH contaminated water were selected for  
216 the DSPE. The prepared Fe<sub>3</sub>O<sub>4</sub>/GO exhibits excellent adsorption efficiency due to the π-

217  $\pi$  stacking of the hydrophobic interaction. Under optimized conditions, the final results  
218 show that PAH recovery remains in between 76.8–103.2%, with 1.7% to 11.7 % of relative  
219 standard deviations. Furthermore, the detection limit was between t 0.09 to 0.19 ng mL<sup>-1</sup>  
220 (Fig. 4).

## 221 **2.2. CNT-based composites**

222 Many studies have investigated the use of graphene oxides and other carbon materials  
223 for environmental remediation of food and biological samples. Especially graphene and  
224 carbon nanotubes (CNT) have been assessed for adsorptive removal of hydrocarbon  
225 compounds, dyes, and metals (Jon et al., 2019). The functionalization of carbon materials  
226 with some good ionic liquids generates CNM/ILs, which are the promising sorbent  
227 materials with high selectivity for different pollutants. The viscosity, miscibility, and high  
228 thermal stability of CNM/ILs make them suitable for adsorption because the CNM/ILs  
229 contains organic and ionic moieties in their structure. CNM/ILs are considered excellent  
230 adsorbents for the environmental remediation of different organic pollutants.

231 Carbon nanotubes (CNTs) are one of the allotropic forms of carbon made from graphene  
232 nanosheets. The structure of CNT can be changed to various shapes like one-  
233 dimensional hollow tubular shape. Single wall carbon nanotube (SWCNTs) and multi-  
234 walled carbon nanotube can be designed according to the number of graphene layers.  
235 The adsorption of different environmental pollutants is due to adsorption sites' presence  
236 on the surface of carbon nanotubes (CNTs) (Liang et al., 2014). To change the surface  
237 properties to be more hydrophilic, the base or the sidewall of the carbon nanotubes (CNT)  
238 can be modified with different oxygen-containing functional groups. Also, for enhanced  
239 separation and purification efficiency, the modification of carbon nanotubes to magnetic  
240 material as MCNT is very popular recently. MCNT gives rapid separation in various  
241 environmental media because of their large surface area and recycling property.

242 Magnetic-based carbon nanotubes (CNTs) hybrid material show promising applications,  
243 especially in solid-phase extraction. This is because of their unique physicochemical  
244 properties and well-engineered surface morphology (Li et al., 2019). In the case of  
245 MCNTs hybrid material for solid-phase extraction application, new procedures were  
246 introduced that extended the application's profile to both organic and inorganic pollutants  
247 determinations such as pesticides, foods, chemical pollutants, drugs. In the end, they give

248 fruitful suggestions for future research direction. In another very recent study, multi-walled  
249 carbon nanotubes polyamide-amine dendrimers (PAMAM)) were designed and further  
250 modified with  $\text{Fe}_3\text{O}_4$  nanoparticles to (MMWCNTs). The prepared MMWCNTs were used  
251 in very efficient and sensitive methods for the remediation of polyaromatic hydrocarbons  
252 (PAH) under solid-phase extraction and gas chromatography with quadrupole mass  
253 spectra detector (GC/MS/MS) (Zhou et al., 2021). Different reaction and testing  
254 parameters such as adsorbent dose, generation of PAMAM, adsorption time, pH, elution  
255 volume, time, and humic acid concentration were thoroughly investigated. After  
256 optimization, the concentration of dibenzothiophene, carbazol, and 7-methyl quinoline  
257 range from  $0.005\text{--}20 \mu\text{g L}^{-1}$ , with excellent linearity. Furthermore, the concentration of  
258 about  $0.001\text{--}20 \mu\text{g L}^{-1}$  4-methyldibenzothiophene, 9-methylcarbazole, and 4,6-dimethyl  
259 dibenzothiophene also shows excellent good linearity. In all cases, the correlation  
260 coefficients are high as 0.996. The sharp recoveries were noted in between 87.0% to  
261 15.1%. The given results concluded that this is a reliable method and can be used to  
262 remove aromatic poly hydrocarbons from different wastewater samples.

263 A collection of many studies was reported for the remediation of many inorganic and  
264 organic pollutants while using magnetic carbon nanotubes (MCNTs). First, the  
265 environmental effects of different trace and toxic metals, different dyes were discussed in  
266 detail. The contamination of these pollutants severely impacts both humans and plants  
267 and can be carcinogenic and harmful to nature. Therefore, priority is given to remove  
268 these toxic pollutants from the different environmental media (Khan et al., 2021e). Carbon  
269 nanotubes (CNTs) give the possible solution to remove toxic metal and dyes from  
270 wastewater, further modifying CNTs with  $\text{Fe}_3\text{O}_4$  nanoparticles to design new magnetic  
271 carbon nanotube MCNTs hybrid materials make this emerging material as an adsorbent  
272 more applicable. The remarkable properties of magnetic carbon nanotube such as easy  
273 separation procedure, reusability, large surface area, and surface to volume ratio  
274 increase the importance of these materials for the rapid removal of trace metals and  
275 different kinds of dyes (Fig. 5). Buckypaper (BP) as separation membranes also give  
276 excellent results like magnetic carbon nanotubes (MCNTs), and give favourable  
277 remediation because of their high adsorption, strength, and porosity. The utilization of

278 Buckypaper (BP) membranes s limited to aqueous samples, and their application for dyes  
279 and metals removal is very less.

280 Multi-walled magnetic carbon nanotubes were constructed by the covalent grafting of  $\beta$ -  
281 cyclodextrin on multi-walled carbon nanotubes (MMWCNTs) to develop a novel material  
282 named  $\beta$ -CD@Fe<sub>3</sub>O<sub>4</sub>/MWCNTs. Different high sophisticated instruments characterize the  
283 prepared material such as XRD, FT-IR, Raman Spectroscopy, SEM, TGA, surface area  
284 (BET) VSM. $\beta$ -CD@Fe<sub>3</sub>O<sub>4</sub>/MWCNT has a large pore volume and surface area.  
285 Furthermore, the application for the removal of Ni ions is excellent at optimized conditions  
286 such as pH, adsorption time, and temperature (Lin et al., 2021). Also, the adsorption  
287 follows the Langmuir and pseudo-first-order kinetics, and thermodynamically, the process  
288 is exothermic with a maximum of 103 mg/g of Ni<sup>+2</sup> ion on the surface of  $\beta$ -  
289 CD@Fe<sub>3</sub>O<sub>4</sub>/MWCNT at ambient temperature. And $\beta$ -CD@Fe<sub>3</sub>O<sub>4</sub>/MWCNT shows the  
290 recycling capacity of about five times in a row. Therefore, Lin and his coworkers presented  
291 an environment-friendly and novel adsorbent material ( $\beta$ -CD@Fe<sub>3</sub>O<sub>4</sub>/MWCNT) having  
292 the potential to effectively remove Ni<sup>+2</sup> ion from aqueous samples.

### 293 **3. MOF- and COF-based porous magnetic materials as MSPE adsorbents**

294 The most enhanced class of materials for the effective removal of different kinds of  
295 organic and inorganic pollutants are porous hybrid materials such as magnetic MOFs,  
296 Magnetic COFs, and other mesoporous (PCOMS), metal-organic frameworks (MOFs),  
297 and mesoporous materials. These materials show large pore size and surface area with  
298 high adsorption capacity and can be easily modified by grafting magnetic nanoparticles.  
299 Furthermore, the adsorption process can speed up by combining magnetic nanoparticles  
300 and porous material in a single hybrid entity.

#### 301 **3.1. MOF-based magnetic hybrid material**

302 MOFs are composed of (metal ions/clusters) as an inorganic component strongly linked  
303 with organic compounds having carboxylic or nitro-containing functional groups as  
304 organic via strong through a coordinate covalent bond. The coordination of the organic  
305 and inorganic entities leads to various functional materials with some promising properties  
306 and multi-dimensional geometries (Ali et al., 2020e). The solid-phase extraction is  
307 possible on MOFs surface because of the superhydrophobicity of  $\pi$ - $\pi$  bonds (Wen et al.,  
308 2021). Generally, the non-spherical surface morphology of MOFs is the drawback

309 because the separation of MOFs is very difficult from the targeted adhered compound in  
310 the solutions. To solve this problem, the mixing of MOFs and MNPs to prepare strong  
311 MNPs/MOFs can be separated from the aqueous solution through an external magnet  
312 (Jiang et al., 2021). Also, the use of some conventional methods such as filtration and  
313 centrifugation can be avoided. In this part of the review, we discuss the different methods  
314 for the magnetization of MOFs, such as encapsulation, mixing, layer by layer, etc. (Ricco  
315 et al., 2013). Glycopeptides and glycoproteins detection in humans' fluids are important  
316 with clinical importance for the detection of disease biomarkers. However, the interfering  
317 liquids make this quantitative detection with low abundance in humans fluids more  
318 challenging. Therefore, the application of magnetic MOFs as an MSPE is more  
319 advantageous due to their low price, easy preparation, and high magnetic domain (Qi et  
320 al., 2021). Table 2 explains some of the magnetic MOFs as an MSPE adsorbent for the  
321 glycopeptides and glycoproteins.

322 A single step and direct carbonization process was adopted to prepare magnetic porous  
323 carbon (MPC) material leading to the cobalt-metal organic framework (Co-MOF). The  
324 prepared Co-MNPC material were characterized for their structure, surface morphology,  
325 and magnetic domain while using SEM, TEM, XRD VSM, and N<sub>2</sub> adsorption. Co-MNPC  
326 exhibits large pore volume, surface area, and super magnetic properties. Furthermore,  
327 the material was checked for solid-phase extraction applications to remove insecticides  
328 neonicotinoid from the samples of fat melon and water, and the final results were  
329 confirmed by high-performance liquid chromatography. The experimental parameters and  
330 the extraction coefficient were investigated for their possible effects on the whole  
331 remediation process. The final results mentioned the efficient adsorption capacity of  
332 magnetic Co-MNPC material (Hao et al., 2014).

333 Fe<sub>3</sub>O<sub>4</sub>@MOF-808) as a facile MNPs/MOFs was designed and prepared through the  
334 solvothermal method and was employed as a DSPE to remove benzoyl urea (BUs), a  
335 famous insecticide from different juice and tea samples (Jia et al., 2020). The surface  
336 morphology, functional groups, and the magnetic domain were checked through SEM,  
337 FT/IR, XRD, and VSM. Furthermore, a detailed investigation was made for the adsorption  
338 process regarding the amount of adsorbent and extraction time. Also, suitable solvent for  
339 elution, elution time, and volume were also optimized. Fe<sub>3</sub>O<sub>4</sub>@MOF-808 MNPs/MOFs

340 applications are promising because they can be recycled much time without ant decrease  
341 in efficiency. The rapid adsorption process is because of the different attractive forces  
342 between  $\text{Fe}_3\text{O}_4@\text{MOF-808}$  and benzoyl urea (BUs), such as hydrophobic interaction,  $\pi$ -  
343  $\pi$  interactions, and hydrogen bonding. In the end, a very simple and sensitive method  
344 was designed by the connection of HPLC coupling with  $\text{Fe}_3\text{O}_4@\text{MOF-808}$ -based for the  
345 improved MSPE. The detection limits are low, i.e., 0.04 to 0.15 ng/mL, with wide linear  
346 ranges of about 0.15 to 50 ng/mL, and the recovery rate is about 84.6 to 98.3% which is  
347 quite satisfactory (Jia et al., 2020). The proposed  $\text{Fe}_3\text{O}_4@\text{MOF-808}$ ) as an MNPs/MOFs  
348 coupled with HPLC give rapid and safe results as an MSPE tool for the removal of s  
349 benzoyl urea (BUs) BUs from tea and beverages samples.

350  $\text{Fe}_3\text{O}_4@\text{SiO}_2@\text{MOF/TiO}_2$  with core-shell morphology was prepared while using the  
351 encapsulation method and was checked as a suitable adsorbent for MSPE to efficiently  
352 remove triazole fungicides from environmental samples (Su et al., 2016). Five different  
353 triazole fungicides samples as target such as tebuconazole, triadimenol, hexaconazole,  
354 myclobutanil, and diniconazole were used for MSPE. After the adsorption of these  
355 samples on  $\text{Fe}_3\text{O}_4@\text{SiO}_2@\text{MOF/TiO}_2$  microspheres, the adsorbed material was  
356 separated from the adsorbent while using an external magnet. LC/MS was used for the  
357 determination of the desorbed analytes solution in methanol. The final extraction  
358 efficiency was affected by changing some extraction parameters, and response surface  
359 methodology was used to optimize these parameters. The detection and quantification  
360 limits were 0.19 to 1.20  $\text{ngL}^{-1}$  and 0.61 to 3.62  $\text{ng L}^{-1}$ .  $\text{Fe}_3\text{O}_4@\text{SiO}_2@\text{MOF/TiO}_2$  was  
361 successfully used for the fungicide concentration in many environmental wastewater  
362 samples, and it was noted that the method gives a satisfying recovery of up to 90 to 104 %  
363 for four samples and exhibits promising applications as MSPE for the quick removal of  
364 fungicides from wastewater samples.

365 Wang and co-workers reported another very effective magnetic Cu-MOFs magnetic  
366 nanocomposites as MSPE adsorbent. A chemical bonding method was used for the  
367 preparation of  $\text{Fe}_3\text{O}_4$  (MNPs), Cu-MOFs, and graphene oxide (GO). In this method, GO  
368 MNPs and CU-MOFs were loaded onto graphene oxides working as a platform (Fig. 6).  
369 The prepared Magnetic Cu-MOFs composite exhibits a strong magnetic domain with  
370 quick separation and large surface pore size, allowing them as promising adsorbent

371 (Wang et al., 2018a). The silica is working as a shell to protect MNPs from oxidation and  
372 work as a platform to integrate MNPs and GO. The integration process is actually the  
373 silica shells modification by amino group followed by the bonding of amino group and  
374 carboxylic group on the surface of GO sheets. Different techniques were used, such as  
375 SEM, TGA, TEM, XRD, FT-IR, and nitrogen adsorption, to characterize the prepared  
376 Magnetic Cu-MOFs magnetic nanocomposites. Furthermore, the magnetic Cu-MOFs  
377 were checked as MSPE to remediate six different aromatic insecticides from actual  
378 samples, then HPLC was successfully used for the quantification. All experimental  
379 parameters such as extraction temperature and time, oscillation rate, adsorbent amount,  
380 desorption times were optimized for excellent results. Good linearity of more than 0.9931  
381 and relative standard deviations of 1.9 to 2.7% was noted under optimal conditions. Six  
382 insecticide samples were checked, and LOQ and LOD were found as low as 1.0–5.2  $\mu\text{g L}^{-1}$   
383  $^1$  and 0.30–1.58  $\mu\text{g L}^{-1}$ , respectively. Remarkably, the prepared  $\text{Fe}_3\text{O}_4@\text{SiO}_2\text{-GO-MOFs}$   
384 nanocomposites demonstrate promising results for the adsorption of six different  
385 insecticides remediation (Wang et al., 2018b).

386 Peter Behrens prepared MOF-801 for the first time by the strong coordinating covalent  
387 bond between  $\text{Zr}^{4+}$  as central metal ion and fumaric acid as organic ligand. The prepared  
388 MOFs exhibits spherical shape, large surface area, and pore size with three-dimensional  
389 surface morphology. Furthermore, the preparation method of MOF-801 is very simple and  
390 can easily be controlled; MOF-801 shows chemical and thermal stability and pH  
391 resistance (Zahn et al., 2014). Therefore, MOF-801 can be used as a special material for  
392 solid-phase adsorption. To further improve the applications of MOF-801 as an MSPE  
393 material, magnetic MOF-801 was generated by the in-situ growth of MOF-801 on MNPs  
394 surface through amidation reaction. The surface of polyethyleneimine magnetic  
395 nanoparticles (PEI-MNPs) contains an amino group that makes an amidation reaction  
396 with the carboxyl group of fumaric acid as organic ligand. The resulting PEI-  
397 MNPs@MOF-801 MNPs-MOF-801 was characterized while using TEM, FT-IR, XRD,  
398 XPS, and the extraction mechanism was also investigated. The prepared PEI-  
399 MNPs@MOF-801 shows an excellent application for the adsorption of sulindac  
400 indometacin, acemetacin under drug treatment (Wan et al., 2021). MSPE-HPLC-UV  
401 method was used on PEI-MNPs@MOF-801 for human plasma. The extraction

402 performance of MSPE-HPLC-UV shows high extraction efficiency under the optimized  
403 condition with 96 to 118 of enrichment factor, 0.03 to 0.05 ng/mL limit of detections, and  
404  $R \geq 0.9987$  linearity, high level of reproducibility, i.e.,  $RSD \leq 4.30\%$ .

### 405 **3.2. Porous covalent organic materials-based composites**

406 One of the expanded chemistries with 2D and 3D crystalline structures is in the form of  
407 Covalent organic frameworks (COFs) (Diercks et al., 2017). The covalent linkage  
408 constructs the entire body of COFs with a high level of physicochemical properties and  
409 crystallinity (Waller et al., 2016). The reported range of the linkage is from reversible imine  
410 (Uribe-Romo et al., 2009), boroxine (Cote et al., 2005) or hydrazone (Uribe-Romo et al.,  
411 2011) to less reversible dioxin (Zhang et al., 2018), phenazine (Guo et al., 2013), triazine  
412 (Kuhn et al., 2008), oxazole (Wei et al. 2018). In the present research era, we need high  
413 crystallinity and chemical stability in the structures of porous COFs. Specially to focus on  
414 the C=C bond for the construction of COFs, which contains good stability and less  
415 reversibility. To solve the problems of COFs, such as low density and hydrophobicity, the  
416 induction of magnetic nanoparticles in the structure of COFs gives a proper remedy in the  
417 preparation of chemical stable magnetic COFs. The construction of porous covalent  
418 organic framework PCOFs can be divided into four board groups, such as a one-step  
419 method for the synthesis of PCOFs and MNPs, indirect mixing of MNPs and PCOFs, the  
420 deposition of PCOFs on MNPs surfaces, and deposition of MNPs on PCOFs surface,  
421 among all these four methods, the last two methods are mainly used methods (Yu et al.,  
422 2019).

423 Dye is one of the typical pollutants which is a serious environmental problem and threat  
424 to human health. Therefore, the effective remediation of these toxic dyes is one of the  
425 emerging research areas and got attention from scientists. Magnetic porous organic  
426 framework (M-POFs) shows promising applications in the removal of dyes and other  
427 environmental pollutants from wastewater, i.e., as MOP magnetic nanoparticles (Huang  
428 et al., 2019), PANI (Kharazi et al., 2019), PAA (Zhou et al., 2013) and so on (Tables 3  
429 and 4). Hu and co-workers (2020) reported a new magnetic porous covalent organic  
430 framework MPCOFs sorbent material for the fluoroquinolones and  $\beta$ -agonists  
431 enrichment in pork and milk samples. During the enrichment process, the reaction of  
432 amino-modified MNPs and the 1,3,5-tri formyl phloroglucinol as reactive monomers and

433 2,5-diaminobenzenesulfonic acid DABA through Schiff base-condensation reaction  
434 leading to prepare the composite of a porous magnetic covalent organic framework  
435 called TFP-DABA MNS. After the extraction process optimization, and coupling with  
436 HPLC-MS/MS, a reproducible and effective process was developed to quantify the  
437 traces of fluoroquinolones and  $\beta$ -agonists in the selected food sample. The final results  
438 show excellent linearity ( $R^2 \geq 0.9916$ ), as well as low LOQs in the range of 0.1 to 0.2  
439  $\text{ng g}^{-1}$  for both fluoroquinolones and  $\beta$ -agonists (Hu et al., 2020). They also reported a  
440 novel magnetic COFs, having bouquet-shape and composed of a flower-shaped MNPs  
441 and COF stem. The 1,3,5 triformylphoroglucinol monomer was grown on the surface of  
442 amino-functionalized MNPs while using a solution-phase reaction and well structure  
443 magnetic COFs was generated.

444 He et al. (2017) reported a novel magnetic COFs, having bouquet-shape and composed  
445 of a flower-shaped MNPs and COF stem. The 1,3,5 triformylphoroglucinol monomer was  
446 grown on the surface of amino-functionalized MNPs while using a solution-phase  
447 reaction. As a result, well-structured magnetic COFs were generated, which was  
448 mandatory for the subsequent formation of the COFs and directed growth. To effectively  
449 construct the nanofibers of COFs, the surface of MNPs was modified with p-  
450 phenylenediamine at room temperature. The prepared bouquet-shaped magnetic COFs  
451 exhibits large pore volume and surface area, but the BET surface area is low of about  
452  $247.8 \text{ m}^2 \text{ g}^{-1}$ , and this is because of the addition of MNPs. The magnetic domain of the  
453 prepared magnetic COFs are from 40.1 to 69.4  $\text{emu g}^{-1}$ . The magnetic COFs showed  
454 excellent application as a sorbent and was successfully utilized for the extraction of  
455 polyaromatic hydrocarbon (PAHs); this is because of the hydrophobic interactions,  
456 hydrogen bonding. After coupling with HPLC-FID, the material shows low LODs of about  
457 73-110 % and high recovery good recovery of 0.24 to 1.01  $\text{ngL}^{-1}$ . Lu et al. (2020) used a  
458 solvothermal method for the preparation of nitro functionalized magnetic covalent organic  
459 framework ( $\text{Fe}_3\text{O}_4@\text{COF}-(\text{NO}_2)_2$ ) and was tested as adsorbent for the MSPE of  
460 insecticides and neonicotinoid in different vegetable samples. The prepared  
461  $\text{Fe}_3\text{O}_4@\text{COF}-(\text{NO}_2)_2$  functional material shows thermal, chemical stability, and  
462 hydrophilic nature, which help in the MSPE of polar compounds. The strong hydrophilic  
463 interaction of  $\text{Fe}_3\text{O}_4@\text{COF}-(\text{NO}_2)_2$  enriching neonicotinoids very efficiently (Lu et al.,

464 2020). The reported method exhibits a very good linearity of about 0.1 to 30 ng mL<sup>-1</sup>,  
465 followed by a low range of detection limit, which is about 0.02 to 0.05 ng mL<sup>-1</sup>). The  
466 enrichment factors are high in the range of 170 to 250, and the recovery rate is about  
467 77.5% to 110.2%, which is looking satisfactory. The reported results show that the  
468 extraction efficiency increased for different pollutants after the functionalization and  
469 modification of (Fe<sub>3</sub>O<sub>4</sub>@COF-(NO<sub>2</sub>)<sub>2</sub>) (Fig. 7).

### 470 **3.3. Magnetic mesoporous composites materials**

471 Generally, nanoscale mesoporous materials possess pore size in the range of 2- 50 nm  
472 with a unique surface morphology (Zhao et al., 2012). The biocompatibility, promising  
473 structural features, i.e., control particle size, large pore size, and surface area, engineered  
474 mesoporous structure the reported mesoporous materials exhibited high-value  
475 application (Yang et al., 2012). The mesoporous features in the entire structures of the  
476 material create some active sites for effective interactions, making it possible to use these  
477 mesoporous materials for different applications such as sensing, catalysis, adsorption,  
478 and targeted drug delivery. A novel adsorbent was prepared by the fabrication of  
479 aminopropyl and octyl groups onto the surface of magnetic mesoporous silica (mOAS).  
480 In the first stage, the pseudomorphic transformation was used to prepare magnetic  
481 mesoporous silica (Zhu et al., 2012), followed by the surface modification with  
482 aminopropyl and octyl groups. The material was characterized for its surface morphology  
483 and other physical and chemical properties by XRD, SEM, XPS, nitrogen adsorption  
484 (NAM), VSM, and FTIR. Furthermore, the mOAS was checked as sorbents and was  
485 employed for MSPE phenoxy carboxylic acid in different environmental aqueous samples.  
486 Then the detection was confirmed through HPLC-MS/MS having triple-quadrupole  
487 tandem (Zhang et al., 2020a). Finally, MSPE-UHPLC-MS/MS method was optimized and  
488 established for the effective MSPE of phenoxy carboxylic acid in the environmental  
489 sample (Fig. 8). The final results explain the great potential of mOAS has as MSPE  
490 sorbent, especially for acidic pollutants from different wastewater samples.

491 Magnetic nanoparticles were coated with the layer of mesoporous silica modified with  
492 methyl dimethoxy, and p-toluenesulfonic acid (PTSA) was used as a catalyst and finally,  
493 a well defined Fe<sub>3</sub>O<sub>4</sub>/mSiO<sub>2</sub>-Me-PTSA material was prepared (Qin et al., 2018a). The  
494 prepared Fe<sub>3</sub>O<sub>4</sub>/mSiO<sub>2</sub>-Me-PTSA material was used as MSPE sorbent for the efficient

495 removal of polychlorinated biphenyls from wastewater samples. The sol-gel process was  
496 used for the synthesis of  $\text{Fe}_3\text{O}_4/\text{mSiO}_2$  as magneto porous silica. In the process,  
497 cetyltrimethylammonium bromide (CTAB) was used as a surfactant and silica (TEOS) as  
498 a precursor. Then the surface of  $\text{Fe}_3\text{O}_4/\text{mSiO}_2$  was coated with methyl dimethoxy. p-  
499 toluenesulfonic acid PTSA was used as a catalyst to speed up the reaction. The  
500  $\text{Fe}_3\text{O}_4/\text{mSiO}_2\text{-Me-PTSA}$  exhibits a strong magnetic domain of about  $33 \text{ emug}^{-1}$  and a  
501 large surface area of about  $197.1 \text{ m}^2 \text{ g}^{-1}$  and, therefore, gives a very quick magnetic  
502 separation. Also, the adsorption time of the targeted polychlorinated biphenyls is about  
503 10 min. Furthermore, the polychlorinated biphenyls enrichment factors are very high from  
504 119 to 147, and the adsorption efficiency of the  $\text{Fe}_3\text{O}_4/\text{mSiO}_2\text{-Me-PTSA}$  for  
505 polychlorinated biphenyls was noted as  $46.3 \text{ mg g}^{-1}$ . Therefore, the reported method  
506 shows promising results with 85.25-118.60% recoveries and low LODs, which is about  
507  $0.16\text{-}0.91 \text{ ng L}^{-1}$  (Qin et al., 2018b).

508 In another study,  $\text{Fe}_3\text{O}_4@\text{RF}@\text{mTiO}_2$  with proper core-shell like surface morphology was  
509 designed and prepared and tested as MSPE sorbent for the effective removal of arsenic  
510 from highly acidic samples. The surface  $\text{Fe}_3\text{O}_4$  was first fabricated with resorcinol-  
511 formaldehyde (RF) followed by mesoporous  $\text{TiO}_2$  with a shell thickness of about 50 nm  
512 and a surface area of about  $337 \text{ m}^2 \text{ g}^{-1}$ , and a large pore volume of  $0.42 \text{ cm}^3 \text{ g}^{-1}$ . The  
513 prepared  $\text{Fe}_3\text{O}_4@\text{RF}@\text{mTiO}_2$  material gives quick adsorption ( $1.16 \text{ g mg}^{-1} \text{ h}^{-1}$ ) and 139  
514  $\text{mg g}^{-1}$  adsorption capacity, which was calculated through the Langmuir model at pH in  
515 the range of 3 to 3.5. The entire structure of the  $\text{Fe}_3\text{O}_4@\text{RF}@\text{mTiO}_2$  is composed of 130  
516 nm of  $\text{Fe}_3\text{O}_4$  inner core and 50 nm of  $\text{RF}@\text{mTiO}_2$  shell, which makes this material strongly  
517 magnetic and can be separated while using an external magnetic field and can be  
518 recycled many times. Moreover, the resorcinol-formaldehyde shows hydrophobic nature  
519 and makes about 10 nm shell and helping the entire  $\text{Fe}_3\text{O}_4$  core from etching against acid  
520 solution (Zhao et al., 2018). Also, in the adsorption process,  $\text{Fe}_3\text{O}_4@\text{RF}@\text{mTiO}_2$  core-  
521 shell material shows some surface complexation and electrostatic forces between  $\text{TiO}_2$   
522 crystals arsenate and hence can be used as promising multi-layer material for wastewater  
523 treatment in the long run.

#### 524 **4. Other magnetic composites as MSPE adsorbents**

525 Along with those above magnetic hybrid materials, MNPs can be fabricated by coupling  
526 with some other functionalized materials, including metallic nanomaterials, silicon,  
527 chitosan, and surfactants, to prepared excellent MSPE sorbents. The summary of some  
528 other magnetic hybrid MSPE sorbents for the remediation of environmental pollutants is  
529 mentioned in Table 5. Silica and silicon magnetic materials show promising applications  
530 as MSPE due to some unique features such as easy surface modification, availability,  
531 low cost, mechanical stability. Because of these unique properties, magnetic silicon  
532 materials exhibit excellent adsorption applications. Three different cores, i.e.,  $\gamma$ - $\text{Fe}_2\text{O}_3$ ,  
533  $\text{MnFe}_2\text{O}_4$ , and  $\text{CoFe}_2\text{O}_4$ , were successfully fabricated with a modified silica shell followed  
534 by alkyl modification and were used for the MSPE sorbent of triclosan under  
535 environmentally friendly and one-pot process. The prepared  $\gamma$ - $\text{Fe}_2\text{O}_3$ @ $\text{SiO}_2$  and  $\gamma$ -  
536  $\text{Fe}_2\text{O}_3$ @ $\text{SiO}_2$ -C18 material was characterized through VSM, TGA, XRD, FTIR, BET area,  
537 DLS, contact angle, and zeta potential. All three magnetic materials show cores shell  
538 surface morphology and hydrophobic wettability. The shell thickness is about 2 nm. The  
539 magnetic core is about 13 nm with effective organofunctionalization and shows effective  
540 adsorption of triclosan (Caon et al., 2020). Furthermore, after coupling with HPLC, the  
541 results revealed that the 0.4–102.4  $\mu\text{g L}^{-1}$  linear range,  $R^2 > 0.99$  of very good linearity,  
542 and the quantification limit detection of about 0.36 to 1.20  $\mu\text{g L}^{-1}$ , noted respectively. The  
543 prepared magnetic nano adsorbent as MSPE can be reused with high efficiency under  
544 the 4.76 signal enhancement (Fig. 9).

545 In another study, a novel  $\text{Fe}_3\text{O}_4$ @ $\text{SiO}_2$ - $\text{NH}_2$ / $\text{F}_{13}$  magnetic silica hybrid material was  
546 prepared through a one-step reaction. First, the surface of  $\text{SiO}_2$  was modified with an  
547 amino group and the chain of octyl-perfluorinated while using the sol-gel procedure (Zhou  
548 et al., 2016a). After the complete experiment, the prepared  $\text{Fe}_3\text{O}_4$ @ $\text{SiO}_2$ - $\text{NH}_2$ / $\text{F}_{13}$  material  
549 shows excellent adsorption of perfluorinated compounds from the selected water samples  
550 and the results was further confirmed through HPLC-MS/MS. For example, in a 500 mL  
551 water sample, 50 mg of  $\text{Fe}_3\text{O}_4$ @ $\text{SiO}_2$ - $\text{NH}_2$ / $\text{F}_{13}$  as MSPE sorbent was dispersed, and  
552 within 30 min, the adsorption equilibrium was reached. The high adsorption efficiency is  
553 because of the fluorine-fluorine (F-F) interactions and high electrostatic attraction followed  
554 by the size exclusion effect. The noted recoveries were 90.65 to 106.67% and 0.029-  
555 0.099  $\text{ng L}^{-1}$  of low LODs. Therefore  $\text{Fe}_3\text{O}_4$ @ $\text{SiO}_2$ - $\text{NH}_2$ / $\text{F}_{13}$  composite can be extensively

556 applied as a useful adsorbent, particularly for aqueous solutions with large volume, to rate  
557 the concentration levels of average PFCs in environmental water systems (Zhou et al.,  
558 2016a).

559 The composites of natural polymers such as chitosan with MNPs also show promising  
560 applications as an MSPE sorbent. Chitosan is a well-known natural polymer with amino  
561 and carboxylic groups on its surface, which import some excellent properties such as  
562 biodegradability and biocompatibility followed by simple modification (Khan et al., 2019;  
563 Khan et al., 2020b; Aziz et al., 2020; Ali et al., 2020d). More recently, generating magnetic  
564 chitosan hybrid material was designed and fabricated by the dispersion ferrites of the  
565 entire chitosan matrix, giving the microspheres of ternary ferrites chitosan (TFCM)  
566 (Nawaz et al., 2020; Ali et al., 2018). The co-precipitation method was used to prepare  
567 the nanoparticles of ternary ferrites, followed by the induction of chitosan matrix to  
568 synthesize magnetic chitosan as an effective adsorbent for methylene blue dye. The  
569 composition of the design photocatalysis ( $\text{Fe}_2\text{Zn}_{0.5}\text{Ni}_{0.5}\text{O}_4$ ). The crystalline nature of the  
570 magnetic chitosan material is because of the inside metals, which are helping in the redox  
571 coupling and decrease the effect of recombination of the conduction and valance bands  
572 (Nawaz et al., 2020).

573 Generally, the induction of chitosan effectively assists the growth of MNPs but also stop  
574 their accumulation. Tolessa et al. fabricated magnetic chitosan hybrid materials in the  
575 size of 2  $\mu\text{m}$  through suspension cross-linking method as used as MSPE sorbent to  
576 remove silver (Ag) nanoparticles (Tolessa et al., 2017). Their study dispersed MNPs in  
577 1% chitosan; next, toluene was added to the mixture containing the Span-80 emulsifier.  
578 Then the mixture was stirred at 500 rpm for 30 min; during this process, NaOH and  
579 glutaraldehyde solution was eventually added. In the end, external magnetic was to  
580 separate magnetic chitosan composite material. After coupling with ICP-MS (inductively  
581 combined plasma-mass spectrometry), the LODs are low with different size and coating  
582 for three Ag particles, i.e., 0.016-0.023  $\mu\text{g/L}$ . The high extraction efficiency of silver (Ag)  
583 nanoparticles is because of the positive charges on the chitosan surface, making them a  
584 good adsorbent. The extraction efficiency was reported in the range of 84.9 to 98.8%,  
585 which shows negative charges because of organic matter coating onto their surface (Fig.

586 10). The prepared magnetic chitosan hybrid material can be reused, and the efficiency  
587 remains about 77.2 + 2.2% after three-time recycling.

## 588 **5. Conclusions and perspectives**

589 In this current article, we summarized the progress and development in the field of MSPE  
590 sorbents and their effective usage as an adsorbent for the extraction of many  
591 environmental toxic pollutants such as organic solvents, dyes, and trace metals. The main  
592 toxic and dangerous pollutants which are found in the biological, environmental, and food  
593 matrix are heavy metals, drugs residue, pesticides, pesticides, phthalate esters,  
594 polyaromatic hydrocarbons, polychlorinated biphenyls, bisphenol A, perfluorinated  
595 compounds. Due to their diverse surface morphology, structure, and physicochemical  
596 properties, the MSPE sorbents material needs accurate design and fabrication for their  
597 promising extraction applications. Magnetic solid-phase extraction shows superior  
598 adsorption advantages over simple conventional solid-phase extraction because of  
599 integrating the magnetic components. The magnetic domain imports some good  
600 properties to prepared MSPE sorbent material, such as high adsorption sites, large  
601 surface area, mechanical and chemical stability, and quick separation by the external  
602 magnetic field from the complex sample matrix. Therefore, the induction of magnetic  
603 components makes this MSPE sorbent material more promising after coupling with  
604 suitable detection techniques and can be employed for quantitative and qualitative  
605 analysis of trace pollutants.

606 In the near future, to utilize more MSPEs sorbent as a versatile material, need more efforts  
607 in the direction to overcome some of the limitations facing during the design and  
608 fabrication process, MSPE adsorption process, and then their practical application.  
609 Therefore, in the first step, we need to identify the problem, such as overcoming the poor  
610 chemical stability, heterogeneous shapes, dispersibility, and recycling in harsh  
611 environmental conditions. Furthermore, it is needed to simplify the synthesis and  
612 fabrication strategies with optimization and use fewer harmful reagents. Also, to explore  
613 some novel environment-friendly materials to reduce harmful effects and the  
614 contamination of MSPEs sorbent material and further introduce green chemistry. Need  
615 main focus to generate some new applications of these MSPEs sorbents by coupling with  
616 suitable analytical techniques. The objective should be to achieve miniaturization,

617 automation, and clear sample analysis with high throughput to get a fast, portable, and  
618 satisfactory application. Solving these problems will make the utilization of these MSPEs  
619 sorbent materials eventually lead us to remarkable progress for sample pretreatment.

## 620 **Acknowledgments**

621 Consejo Nacional de Ciencia y Tecnología (CONACYT) is thankfully acknowledged for  
622 partially supporting this work under Sistema Nacional de Investigadores (SNI) program  
623 awarded to Hafiz M.N. Iqbal (CVU: 735340).

## 624 **Conflict of interests**

625 The author(s) declare no conflicting interests.

## 626 **References**

- 627 Ahmad, W., Khan, A., Ali, N., Khan, S., Uddin, S., Malik, S., ... & Bilal, M. (2021).  
628 Photocatalytic degradation of crystal violet dye under sunlight by chitosan-  
629 encapsulated ternary metal selenide microspheres. *Environmental Science and*  
630 *Pollution Research*, 28(7), 8074-8087.
- 631 Akbarzade, S., CHamsaz, M., & Rounaghi, G. H. (2018). Highly selective  
632 preconcentration of ultra-trace amounts of lead ions in real water and food samples  
633 by dispersive solid phase extraction using modified magnetic graphene oxide as a  
634 novel sorbent. *Analytical Methods*, 10(18), 2081-2087.
- 635 Ali, F., Ibrahim, M., Khan, F., Bibi, I., & Shah, S. W. (2018). Binding affinities of cationic  
636 dyes in the presence of activated charcoal and anionic surfactant in the premicellar  
637 region. *Materials Research Express*, 5(3), 035405.
- 638 Ali, N., Zaman, H., Bilal, M., Nazir, M. S., & Iqbal, H. M. (2019). Environmental  
639 perspectives of interfacially active and magnetically recoverable composite  
640 materials—a review. *Science of the total environment*, 670, 523-538.
- 641 Ali, N., Bilal, M., Khan, A., Ali, F., & Iqbal, H. M. (2020a). Effective exploitation of anionic,  
642 nonionic, and nanoparticle-stabilized surfactant foams for petroleum hydrocarbon  
643 contaminated soil remediation. *Science of the Total Environment*, 704, 135391.
- 644 Ali, N., Ali, F., Said, A., Begum, T., Bilal, M., Rab, A., ... & Ahmad, I. (2020b).  
645 Characterization and deployment of surface-engineered cobalt ferrite nanospheres  
646 as photocatalyst for highly efficient remediation of alizarin red S dye from aqueous

647 solution. *Journal of Inorganic and Organometallic Polymers and Materials*, 30(12),  
648 5063-5073.

649 Ali, N., Khan, A., Bilal, M., Malik, S., Badshah, S., & Iqbal, H. (2020c). Chitosan-based  
650 bio-composite modified with thiocarbamate moiety for decontamination of cations  
651 from the aqueous media. *Molecules*, 25(1), 226.

652 Ali, N., Bilal, M., Khan, A., Ali, F., Khan, H., Khan, H. A., ... & Iqbal, H. M. (2020d).  
653 Understanding the hierarchical assemblies and oil/water separation applications of  
654 metal-organic frameworks. *Journal of Molecular Liquids*, 114273.

655 Ali, N., Zhang, B., Zhang, H., Li, W., Zaman, W., Tian, L., & Zhang, Q. (2015a). Novel  
656 Janus magnetic micro particle synthesis and its applications as a demulsifier for  
657 breaking heavy crude oil and water emulsion. *Fuel*, 141, 258-267.

658 Ali, N., Zhang, B., Zhang, H., Zaman, W., Li, X., Li, W., & Zhang, Q. (2015b). Interfacially  
659 active and magnetically responsive composite nanoparticles with raspberry like  
660 structure; synthesis and its applications for heavy crude oil/water separation. *Colloids  
661 and Surfaces A: Physicochemical and Engineering Aspects*, 472, 38-49.

662 Ali, N., Zhang, B., Zhang, H., Zaman, W., Ali, S., Ali, Z., ... & Zhang, Q. (2015c).  
663 Monodispers and multifunctional magnetic composite core shell microspheres for  
664 demulsification applications. *Journal of the Chinese Chemical Society*, 62(8), 695-  
665 702.

666 Ali, N., Baoliang, Z., Zhang, H., Zaman, W., Ali, S., Ali, Z., ... & Zhang, Q. (2015d). Iron  
667 oxide-based polymeric magnetic microspheres with a core shell structure: from  
668 controlled synthesis to demulsification applications. *Journal of Polymer  
669 Research*, 22(11), 1-12.

670 Amiri, A., Baghayeri, M., & Sedighi, M. (2018). Magnetic solid-phase extraction of  
671 polycyclic aromatic hydrocarbons using a graphene oxide/Fe<sub>3</sub>O<sub>4</sub>@ polystyrene  
672 nanocomposite. *Microchimica Acta*, 185(8), 1-9.

673 Arabi, M., Ghaedi, M., & Ostovan, A. (2017). Development of a lower toxic approach  
674 based on green synthesis of water-compatible molecularly imprinted nanoparticles  
675 for the extraction of hydrochlorothiazide from human urine. *ACS Sustainable  
676 Chemistry & Engineering*, 5(5), 3775-3785.

677 Ariffin, M. M., Azmi, A. H. M., Saleh, N. M., Mohamad, S., & Rozi, S. K. M. (2019).  
678 Surfactant functionalisation of magnetic nanoparticles: A greener method for  
679 parabens determination in water samples by using magnetic solid phase  
680 extraction. *Microchemical Journal*, 147, 930-940.

681 Aziz, A., Ali, N., Khan, A., Bilal, M., Malik, S., Ali, N., & Khan, H. (2020). Chitosan-zinc  
682 sulfide nanoparticles, characterization and their photocatalytic degradation efficiency  
683 for azo dyes. *International journal of biological macromolecules*, 153, 502-512.

684 Azzouz, A., Kailasa, S. K., Lee, S. S., Rascón, A. J., Ballesteros, E., Zhang, M., & Kim,  
685 K. H. (2018). Review of nanomaterials as sorbents in solid-phase extraction for  
686 environmental samples. *TrAC Trends in Analytical Chemistry*, 108, 347-369.

687 Bagheri, A. R., Arabi, M., Ghaedi, M., Ostovan, A., Wang, X., Li, J., & Chen, L. (2019).  
688 Dummy molecularly imprinted polymers based on a green synthesis strategy for  
689 magnetic solid-phase extraction of acrylamide in food samples. *Talanta*, 195, 390-  
690 400.

691 Cai, M. Q., Su, J., Hu, J. Q., Wang, Q., Dong, C. Y., Pan, S. D., & Jin, M. C. (2016). Planar  
692 graphene oxide-based magnetic ionic liquid nanomaterial for extraction of  
693 chlorophenols from environmental water samples coupled with liquid  
694 chromatography–tandem mass spectrometry. *Journal of Chromatography A*, 1459,  
695 38-46.

696 Caon, N. B., dos Santos Cardoso, C., Faita, F. L., Vitali, L., & Parize, A. L. (2020).  
697 Magnetic solid-phase extraction of triclosan from water using n-octadecyl modified  
698 silica-coated magnetic nanoparticles. *Journal of Environmental Chemical  
699 Engineering*, 8(4), 104003.

700 Clarke, B. O., & Smith, S. R. (2011). Review of 'emerging' organic contaminants in  
701 biosolids and assessment of international research priorities for the agricultural use  
702 of biosolids. *Environment international*, 37(1), 226-247.

703 Changfen, B., Ye, Y., Yuran, T., Wu, J., Yulu, L., Li, Y., ... & Yukui, Z. (2020). Facile  
704 synthesis of hydrophilic magnetic graphene nanocomposites via dopamine self-  
705 polymerization and Michael addition for selective enrichment of N-linked  
706 glycopeptides. *Scientific Reports (Nature Publisher Group)*, 10(1).

707 Chen, H., Li, Y., Wu, H., Sun, N., & Deng, C. (2019a). Smart hydrophilic modification of  
708 magnetic mesoporous silica with zwitterionic L-cysteine for endogenous  
709 glycopeptides recognition. *ACS Sustainable Chemistry & Engineering*, 7(2), 2844-  
710 2851.

711 Chen, Y., Zhang, W., Zhang, Y., Deng, Z., Zhao, W., Du, H., ... & Zhang, S. (2018). In  
712 situ preparation of core-shell magnetic porous aromatic framework nanoparticles for  
713 mixed-mode solid-phase extraction of trace multitarget analytes. *Journal of*  
714 *Chromatography A*, 1556, 1-9.

715 Chen, Z., Chen, B., He, M., Wang, H., & Hu, B. (2019b). A porous organic polymer with  
716 magnetic nanoparticles on a chip array for preconcentration of platinum (IV), gold (III)  
717 and bismuth (III) prior to their on-line quantitation by ICP-MS. *Microchimica*  
718 *Acta*, 186(2), 107.

719 Cote, A. P., Benin, A. I., Ockwig, N. W., O'Keeffe, M., Matzger, A. J., & Yaghi, O. M.  
720 (2005). Porous, crystalline, covalent organic frameworks. *science*, 310(5751), 1166-  
721 1170.

722 Diercks, C. S., & Yaghi, O. M. (2017). The atom, the molecule, and the covalent organic  
723 framework. *Science*, 355(6328).

724 Ersan, G., Apul, O. G., Perreault, F., & Karanfil, T. (2017). Adsorption of organic  
725 contaminants by graphene nanosheets: A review. *Water research*, 126, 385-398.

726 Fan, Y. H., Zhang, S. W., Qin, S. B., Li, X. S., Zhang, Y., & Qi, S. H. (2017). Facile  
727 preparation of hexadecyl-functionalized magnetic core-shell microsphere for the  
728 extraction of polychlorinated biphenyls in environmental waters. *Analytical and*  
729 *bioanalytical chemistry*, 409(13), 3337-3346.

730 Faraji, M., Shabanian, M., & Aryanasab, F. (2018). Efficient removal of anionic dyes from  
731 aqueous media using newly in situ synthesized triazine-based nitrogen-rich network-  
732 modified magnetic nanoparticles. *Journal of the Iranian Chemical Society*, 15(3), 733-  
733 741.

734 Feizbakhsh, A., & Ehteshami, S. (2016). Polythiophene-chitosan magnetic  
735 nanocomposite as a novel sorbent for disperse magnetic solid phase extraction of  
736 triazine herbicides in aquatic media. *Chromatographia*, 79(17), 1177-1185.

737 Gao, C., Bai, J., He, Y., Zheng, Q., Ma, W., & Lin, Z. (2019). Post-synthetic modification  
738 of phenylboronic acid-functionalized magnetic covalent organic frameworks for  
739 specific enrichment of N-linked glycopeptides. *ACS Sustainable Chemistry &*  
740 *Engineering*, 7(23), 18926-18934.

741 Ghorbani-Kalhor, E., Hosseinzadeh-Khanmiri, R., Babazadeh, M., Abolhasani, J., &  
742 Hassanpour, A. (2015). Synthesis and application of a novel magnetic metal-organic  
743 framework nanocomposite for determination of Cd, Pb, and Zn in baby food  
744 samples. *Canadian Journal of Chemistry*, 93(5), 518-525.

745 Guo, J., Xu, Y., Jin, S., Chen, L., Kaji, T., Honsho, Y., ... & Jiang, D. (2013). Conjugated  
746 organic framework with three-dimensionally ordered stable structure and delocalized  
747  $\pi$  clouds. *Nature communications*, 4(1), 1-8.

748 Han, Q., Wang, Z., Xia, J., Chen, S., Zhang, X., & Ding, M. (2012). Facile and tunable  
749 fabrication of Fe<sub>3</sub>O<sub>4</sub>/graphene oxide nanocomposites and their application in the  
750 magnetic solid-phase extraction of polycyclic aromatic hydrocarbons from  
751 environmental water samples. *Talanta*, 101, 388-395.

752 Hao, L., Wang, C., Wu, Q., Li, Z., Zang, X., & Wang, Z. (2014). Metal-organic framework  
753 derived magnetic nanoporous carbon: novel adsorbent for magnetic solid-phase  
754 extraction. *Analytical chemistry*, 86(24), 12199-12205.

755 He, S., Zeng, T., Wang, S., Niu, H., & Cai, Y. (2017a). Facile synthesis of magnetic  
756 covalent organic framework with three-dimensional bouquet-like structure for  
757 enhanced extraction of organic targets. *ACS applied materials & interfaces*, 9(3),  
758 2959-2965.

759 He, L., Cui, W., Wang, Y., Zhao, W., Xiang, G., Jiang, X., ... & Zhang, S. (2017b).  
760 Polymeric ionic liquid based on magnetic materials fabricated through layer-by-layer  
761 assembly as adsorbents for extraction of pesticides. *Journal of Chromatography*  
762 *A*, 1522, 9-15.

763 He, X., Yang, W., Li, S., Liu, Y., Hu, B., Wang, T., & Hou, X. (2018). An amino-  
764 functionalized magnetic framework composite of type Fe<sub>3</sub>O<sub>4</sub>-NH<sub>2</sub>@ MIL-101 (Cr)  
765 for extraction of pyrethroids coupled with GC-ECD. *Microchimica Acta*, 185(2), 1-8.

766 He, Y., He, M., Nan, K., Cao, R., Chen, B., & Hu, B. (2019). Magnetic solid-phase  
767 extraction using sulfur-containing functional magnetic polymer for high-performance

768 liquid chromatography-inductively coupled plasma-mass spectrometric speciation of  
769 mercury in environmental samples. *Journal of Chromatography A*, 1595, 19-27.

770 He, Y., Li, J., Luo, K., Li, L., Chen, J., & Li, J. (2016). Engineering reduced graphene oxide  
771 aerogel produced by effective  $\gamma$ -ray radiation-induced self-assembly and its  
772 application for continuous oil–water separation. *Industrial & Engineering Chemistry  
773 Research*, 55(13), 3775-3781.

774 Hu, K., Pang, T., Shi, Y., Cheng, J., & Huang, Y. (2020). Facile preparation of a magnetic  
775 porous organic frameworks for highly sensitive determination of eight alkaloids in  
776 urine samples based UHPLC-MS/MS. *Microchemical Journal*, 157, 105048.

777 Hu, K., Shi, Y., Zhu, W., Cai, J., Zhao, W., Zeng, H., ... & Zhang, S. (2021). Facile  
778 synthesis of magnetic sulfonated covalent organic framework composites for  
779 simultaneous dispersive solid-phase extraction and determination of  $\beta$ -agonists and  
780 fluoroquinolones in food samples. *Food Chemistry*, 339, 128079.

781 Hu, W., Zhang, P., Liu, X., Yan, B., Xiang, L., Zhang, J., ... & Zeng, H. (2018). An  
782 amphiphobic graphene-based hydrogel as oil-water separator and oil fence  
783 material. *Chemical Engineering Journal*, 353, 708-716.

784 Huan, W., Zhang, J., Qin, H., Huan, F., Wang, B., Wu, M., Li, J., (2019). Magnetic  
785 nanofiber-based zwitterionic hydrophilic material for selective capture and  
786 identification of glycopeptides. *Nanoscale*, 11, 10952-10960.

787 Huang, J., & Yan, Z. (2018). Adsorption mechanism of oil by resilient graphene aerogels  
788 from oil–water emulsion. *Langmuir*, 34(5), 1890-1898.

789 Huang, L., He, M., Chen, B., Cheng, Q., & Hu, B. (2017). Facile green synthesis of  
790 magnetic porous organic polymers for rapid removal and separation of methylene  
791 blue. *ACS Sustainable Chemistry & Engineering*, 5(5), 4050-4055.

792 Huang, L., Shuai, Q., & Hu, S. (2019). Tannin-based magnetic porous organic polymers  
793 as robust scavengers for methylene blue and lead ions. *Journal of Cleaner  
794 Production*, 215, 280-289.

795 Huo, S. H., An, H. Y., Yu, J., Mao, X. F., Zhang, Z., Bai, L., ... & Zhou, P. X. (2017).  
796 Pyrolytic in situ magnetization of metal-organic framework MIL-100 for magnetic  
797 solid-phase extraction. *Journal of Chromatography A*, 1517, 18-25.

798 Ji, W., Zhang, M., Duan, W., Wang, X., Zhao, H., & Guo, L. (2017). Phytic acid-stabilized  
799 super-amphiphilic Fe<sub>3</sub>O<sub>4</sub>-graphene oxide for extraction of polycyclic aromatic  
800 hydrocarbons from vegetable oils. *Food chemistry*, 235, 104-110.

801 Jia, Y., Wang, Y., Yan, M., Wang, Q., Xu, H., Wang, X., ... & Wang, M. (2020). Fabrication  
802 of iron oxide@ MOF-808 as a sorbent for magnetic solid phase extraction of  
803 benzoylurea insecticides in tea beverages and juice samples. *Journal of*  
804 *Chromatography A*, 1615, 460766.

805 Jiang, H. L., Fu, Q. B., Wang, M. L., Lin, J. M., & Zhao, R. S. (2021). Determination of  
806 trace bisphenols in functional beverages through the magnetic solid-phase extraction  
807 with MOF-COF composite. *Food Chemistry*, 345, 128841.

808 Jon, C. S., Meng, L. Y., & Li, D. (2019). Recent review on carbon nanomaterials  
809 functionalized with ionic liquids in sample pretreatment application. *TrAC Trends in*  
810 *Analytical Chemistry*, 120, 115641.

811 Khan, A., Malik, S., Ali, N., Bilal, M., El-Shazly, M., & Iqbal, H. M. (2021a). Biopolymer-  
812 based sorbents for emerging pollutants. In *Sorbents Materials for Controlling*  
813 *Environmental Pollution* (pp. 463-491). Elsevier.

814 Khan, F. S. A., Mubarak, N. M., Tan, Y. H., Khalid, M., Karri, R. R., Walvekar, R., ... &  
815 Mazari, S. A. (2021e). A comprehensive review on magnetic carbon nanotubes and  
816 carbon nanotube-based buckypaper-heavy metal and dyes removal. *Journal of*  
817 *Hazardous Materials*, 125375.

818 Khan, S., Khan, A., Ali, N., Ahmad, S., Ahmad, W., Malik, S., ... & Bilal, M. (2021b).  
819 Degradation of Congo red dye using ternary metal selenide-chitosan microspheres  
820 as robust and reusable catalysts. *Environmental Technology & Innovation*, 22,  
821 101402.

822 Khan, A., Ali, N., Malik, S., Bilal, M., Munir, H., Ferreira, L. F. R., & Iqbal, H. M. (2021c).  
823 Chitosan-based green sorbents for toxic cations removal. In *Sorbents Materials for*  
824 *Controlling Environmental Pollution* (pp. 323-352). Elsevier.

825 Khan, A., Ali, N., Malik, S., Bilal, M., Munir, H., Ferreira, L. F. R., & Iqbal, H. M. (2021d).  
826 Chitosan-based green sorbents for toxic cations removal. In *Sorbents Materials for*  
827 *Controlling Environmental Pollution* (pp. 323-352). Elsevier.

828 Khan, A., Ali, N., Bilal, M., Malik, S., Badshah, S., & Iqbal, H. (2019). Engineering  
829 functionalized chitosan-based sorbent material: characterization and sorption of toxic  
830 elements. *Applied Sciences*, 9(23), 5138.

831 Khan, H., Gul, K., Ara, B., Khan, A., Ali, N., Ali, N., & Bilal, M. (2020). Adsorptive removal  
832 of acrylic acid from the aqueous environment using raw and chemically modified  
833 alumina: Batch adsorption, kinetic, equilibrium and thermodynamic studies. *Journal*  
834 *of Environmental Chemical Engineering*, 8(4), 103927.

835 Kharazi, P., Rahimi, R., & Rabbani, M. (2019). Copper ferrite-polyaniline nanocomposite:  
836 structural, thermal, magnetic and dye adsorption properties. *Solid State*  
837 *Sciences*, 93, 95-100.

838 Kuhn, P., Antonietti, M., & Thomas, A. (2008). Porous, covalent triazine-based  
839 frameworks prepared by ionothermal synthesis. *Angewandte Chemie International*  
840 *Edition*, 47(18), 3450-3453.

841 Leus, K., Folens, K., Nicomel, N. R., Perez, J. P. H., Filippousi, M., Meledina, M., ... &  
842 Van Der Voort, P. (2018). Removal of arsenic and mercury species from water by  
843 covalent triazine framework encapsulated  $\gamma$ -Fe<sub>2</sub>O<sub>3</sub> nanoparticles. *Journal of*  
844 *hazardous materials*, 353, 312-319.

845 Li, N., Chen, J., & Shi, Y. P. (2017a). Magnetic polyethyleneimine functionalized reduced  
846 graphene oxide as a novel magnetic solid-phase extraction adsorbent for the  
847 determination of polar acidic herbicides in rice. *Analytica chimica acta*, 949, 23-34.

848 Li, N., Wu, D., Hu, N., Fan, G., Li, X., Sun, J., ... & Wu, Y. (2018). Effective enrichment  
849 and detection of trace polycyclic aromatic hydrocarbons in food samples based on  
850 magnetic covalent organic framework hybrid microspheres. *Journal of agricultural*  
851 *and food chemistry*, 66(13), 3572-3580.

852 Li, N., Wu, D., Li, X., Zhou, X., Fan, G., Li, G., & Wu, Y. (2020). Effective enrichment and  
853 detection of plant growth regulators in fruits and vegetables using a novel magnetic  
854 covalent organic framework material as the adsorbents. *Food chemistry*, 306,  
855 125455.

856 Li, Q., Zhan, Z., Jin, S., & Tan, B. (2017b). Wetttable magnetic hypercrosslinked  
857 microporous nanoparticle as an efficient adsorbent for water treatment. *Chemical*  
858 *Engineering Journal*, 326, 109-116.

859 Li, W. K., & Shi, Y. P. (2019). Recent advances and applications of carbon nanotubes-  
860 based composites in magnetic solid-phase extraction. *TrAc Trends in Analytical*  
861 *Chemistry*, 118, 652-665.

862 Li, Y., Yang, C. X., & Yan, X. P. (2017c). Controllable preparation of core-shell magnetic  
863 covalent-organic framework nanospheres for efficient adsorption and removal of  
864 bisphenols in aqueous solution. *Chemical communications*, 53(16), 2511-2514.

865 Li, Y., Qi, L., Shen, Y., & Ma, H. (2014). Facile preparation of surface-exchangeable  
866 core@ shell iron oxide@ gold nanoparticles for magnetic solid-phase extraction: use  
867 of gold shell as the intermediate platform for versatile adsorbents with varying self-  
868 assembled monolayers. *Analytica chimica acta*, 811, 36-42.

869 Liang, R., Hu, Y., & Li, G. (2020). Photochemical synthesis of magnetic covalent organic  
870 framework/carbon nanotube composite and its enrichment of heterocyclic aromatic  
871 amines in food samples. *Journal of Chromatography A*, 1618, 460867.

872 Liang, X., Liu, S., Wang, S., Guo, Y., & Jiang, S. (2014). Carbon-based sorbents: carbon  
873 nanotubes. *Journal of Chromatography A*, 1357, 53-67.

874 Liao, Y., Li, J., & Thomas, A. (2017). General route to high surface area covalent organic  
875 frameworks and their metal oxide composites as magnetically recoverable  
876 adsorbents and for energy storage. *ACS Macro Letters*, 6(12), 1444-1450.

877 Lim, M. Y., Choi, Y. S., Shin, H., Kim, K., Shin, D. M., & Lee, J. C. (2018). Cross-linked  
878 graphene oxide membrane functionalized with self-cross-linkable and bactericidal  
879 cardanol for oil/water separation. *ACS Applied Nano Materials*, 1(6), 2600-2608.

880 Lingamdinne, L. P., Koduru, J. R., & Karri, R. R. (2019). A comprehensive review of  
881 applications of magnetic graphene oxide-based nanocomposites for sustainable  
882 water purification. *Journal of environmental management*, 231, 622-634.

883 Lin, S., Zou, C., Liang, H., Peng, H., & Liao, Y. (2021). The effective removal of nickel  
884 ions from aqueous solution onto magnetic multi-walled carbon nanotubes modified  
885 by  $\beta$ -cyclodextrin. *Colloids and Surfaces A: Physicochemical and Engineering*  
886 *Aspects*, 126544.

887 Liu, D., Huang, Z., Li, M., Sun, P., Yu, T., & Zhou, L. (2019). Novel porous magnetic  
888 nanospheres functionalized by  $\beta$ -cyclodextrin polymer and its application in organic  
889 pollutants from aqueous solution. *Environmental Pollution*, 250, 639-649.

890 Liu, H., Zhang, J., Gan, N., Chen, Y., Huang, J., Cao, Y., ... & Lan, H. (2016). Application  
891 of a multifunctional magnetic mesoporous material for seafood sample clean-up prior  
892 to the determination of highly chlorinated polychlorinated biphenyls. *RSC*  
893 *advances*, 6(1), 183-189.

894 Liu, X., Sun, Z., Chen, G., Zhang, W., Cai, Y., Kong, R., ... & You, J. (2015). Determination  
895 of phthalate esters in environmental water by magnetic Zeolitic Imidazolate  
896 Framework-8 solid-phase extraction coupled with high-performance liquid  
897 chromatography. *Journal of Chromatography A*, 1409, 46-52.

898 Liu, Y., Huang, H., Gan, D., Guo, L., Liu, M., Chen, J., ... & Wei, Y. (2018a). A facile  
899 strategy for preparation of magnetic graphene oxide composites and their potential  
900 for environmental adsorption. *Ceramics International*, 44(15), 18571-18577.

901 Liu, Y., Fan, X., Jia, X., Chen, X., Zhang, A., Zhang, B., & Zhang, Q. (2018b). Preparation  
902 of magnetic hyper-cross-linked polymers for the efficient removal of antibiotics from  
903 water. *ACS Sustainable Chemistry & Engineering*, 6(1), 210-222.

904 Lu, J., Wang, R., Luan, J., Li, Y., He, X., Chen, L., & Zhang, Y. (2020). A functionalized  
905 magnetic covalent organic framework for sensitive determination of trace  
906 neonicotinoid residues in vegetable samples. *Journal of Chromatography A*, 1618,  
907 460898.

908 Luo, B., Chen, Q., He, J., Li, Z., Yu, L., Lan, F., & Wu, Y. (2019). Boronic acid-  
909 functionalized magnetic metal-organic frameworks via a dual-ligand strategy for  
910 highly efficient enrichment of phosphopeptides and glycopeptides. *ACS Sustainable*  
911 *Chemistry & Engineering*, 7(6), 6043-6052.

912 Ma, J., Yao, Z., Hou, L., Lu, W., Yang, Q., Li, J., & Chen, L. (2016a). Metal organic  
913 frameworks (MOFs) for magnetic solid-phase extraction of pyrazole/pyrrole  
914 pesticides in environmental water samples followed by HPLC-DAD  
915 determination. *Talanta*, 161, 686-692.

916 Ma, S., He, M., Chen, B., Deng, W., Zheng, Q., & Hu, B. (2016b). Magnetic solid phase  
917 extraction coupled with inductively coupled plasma mass spectrometry for the  
918 speciation of mercury in environmental water and human hair samples. *Talanta*, 146,  
919 93-99.

920 Ma, J., Wu, G., Li, S., Tan, W., Wang, X., Li, J., & Chen, L. (2018). Magnetic solid-phase  
921 extraction of heterocyclic pesticides in environmental water samples using metal-  
922 organic frameworks coupled to high performance liquid chromatography  
923 determination. *Journal of Chromatography A*, 1553, 57-66.

924 Mehdinia, A., Roohi, F., & Jabbari, A. (2011). Rapid magnetic solid phase extraction with  
925 in situ derivatization of methylmercury in seawater by Fe<sub>3</sub>O<sub>4</sub>/polyaniline  
926 nanoparticle. *Journal of Chromatography A*, 1218(28), 4269-4274.

927 Mehdinia, A., Khodaei, N., & Jabbari, A. (2015). Fabrication of graphene/Fe<sub>3</sub>O<sub>4</sub>@  
928 polythiophene nanocomposite and its application in the magnetic solid-phase  
929 extraction of polycyclic aromatic hydrocarbons from environmental water  
930 samples. *Analytica chimica acta*, 868, 1-9.

931 Nawaz, A., Khan, A., Ali, N., Ali, N., & Bilal, M. (2020). Fabrication and characterization  
932 of new ternary ferrites-chitosan nanocomposite for solar-light driven photocatalytic  
933 degradation of a model textile dye. *Environmental Technology & Innovation*, 20,  
934 101079.

935 Nodeh, H. R., Ibrahim, W. A. W., Kamboh, M. A., & Sanagi, M. M. (2017). New magnetic  
936 graphene-based inorganic-organic sol-gel hybrid nanocomposite for simultaneous  
937 analysis of polar and non-polar organophosphorus pesticides from water samples  
938 using solid-phase extraction. *Chemosphere*, 166, 21-30.

939 Ötles, S., & Kartal, C. (2016). Solid-Phase Extraction (SPE): Principles and applications  
940 in food samples. *Acta Scientiarum Polonorum Technologia Alimentaria*, 15(1), 5-15.

941 Pan, L., Xu, M. Y., Liu, Z. L., Du, B. B., Yang, K. H., Wu, L., ... & He, Y. J. (2016). Facile  
942 method for the synthesis of Fe<sub>3</sub>O<sub>4</sub>@ HCP core-shell porous magnetic microspheres  
943 for fast separation of organic dyes from aqueous solution. *RSC advances*, 6(53),  
944 47530-47535.

945 Pan, S., Chen, X., Li, X., & Jin, M. (2019). Nonderivatization method for determination of  
946 glyphosate, glufosinate, bialaphos, and their main metabolites in environmental  
947 waters based on magnetic metal-organic framework pretreatment. *Journal of*  
948 *separation science*, 42(5), 1045-1050.

949 Pastor-Belda, M., Marín-Soler, L., Campillo, N., Viñas, P., & Hernández-Córdoba, M.  
950 (2018). Magnetic carbon nanotube composite for the preconcentration of parabens

951 from water and urine samples using dispersive solid phase extraction. *Journal of*  
952 *Chromatography A*, 1564, 102-109.

953 Pinsrithong, S., & Bunkoed, O. (2018). Hierarchical porous nanostructured polypyrrole-  
954 coated hydrogel beads containing reduced graphene oxide and magnetite  
955 nanoparticles for extraction of phthalates in bottled drinks. *Journal of*  
956 *Chromatography A*, 1570, 19-27.

957 Qi, H., Jiang, L., & Jia, Q. (2021). Application of magnetic solid phase extraction in  
958 separation and enrichment of glycoproteins and glycopeptides. *Chinese Chemical*  
959 *Letters*.

960 Qi, P., Liang, Z. A., Xiao, J., Liu, J., Zhou, Q. Q., Zheng, C. H., ... & Zhang, X. W. (2016).  
961 Mixed hemimicelles solid-phase extraction based on sodium dodecyl sulfate-coated  
962 nano-magnets for selective adsorption and enrichment of illegal cationic dyes in food  
963 matrices prior to high-performance liquid chromatography-diode array detection  
964 detection. *Journal of Chromatography A*, 1437, 25-36.

965 Qi, X., Gao, S., Ding, G., & Tang, A. N. (2017). Synthesis of surface Cr (VI)-imprinted  
966 magnetic nanoparticles for selective dispersive solid-phase extraction and  
967 determination of Cr (VI) in water samples. *Talanta*, 162, 345-353.

968 Qin, S. B., Fan, Y. H., Li, X. S., Zhang, Y., & Qi, S. H. (2018a). Rapid preparation of  
969 methyltrimethoxy-modified magnetic mesoporous silica as an effective solid-phase  
970 extraction adsorbent. *Journal of separation science*, 41(3), 669-677.

971 Qin, S. B., Fan, Y. H., Mou, X. X., Li, X. S., & Qi, S. H. (2018b). Preparation of phenyl-  
972 modified magnetic silica as a selective magnetic solid-phase extraction adsorbent for  
973 polycyclic aromatic hydrocarbons in soils. *Journal of Chromatography A*, 1568, 29-  
974 37.

975 Ren, J. Y., Wang, X. L., Li, X. L., Wang, M. L., Zhao, R. S., & Lin, J. M. (2018). Magnetic  
976 covalent triazine-based frameworks as magnetic solid-phase extraction adsorbents  
977 for sensitive determination of perfluorinated compounds in environmental water  
978 samples. *Analytical and bioanalytical chemistry*, 410(6), 1657-1665.

979 Rezvani-Eivari, M., Amiri, A., Baghayeri, M., & Ghaemi, F. (2016). Magnetized graphene  
980 layers synthesized on the carbon nanofibers as novel adsorbent for the extraction of

981 polycyclic aromatic hydrocarbons from environmental water samples. *Journal of*  
982 *Chromatography A*, 1465, 1-8.

983 Ricco, R., Malfatti, L., Takahashi, M., Hill, A. J., & Falcaro, P. (2013). Applications of  
984 magnetic metal–organic framework composites. *Journal of Materials Chemistry*  
985 *A*, 1(42), 13033-13045.

986 Rocío-Bautista, P., Pino, V., Ayala, J. H., Pasán, J., Ruiz-Pérez, C., & Afonso, A. M.  
987 (2016). A magnetic-based dispersive micro-solid-phase extraction method using the  
988 metal-organic framework HKUST-1 and ultra-high-performance liquid  
989 chromatography with fluorescence detection for determining polycyclic aromatic  
990 hydrocarbons in waters and fruit tea infusions. *Journal of Chromatography A*, 1436,  
991 42-50.

992 Shah, J., & Jan, M. R. (2018). Magnetic chitosan graphene oxide composite for solid  
993 phase extraction of phenylurea herbicides. *Carbohydrate polymers*, 199, 461-472.

994 Sha, O., Wang, Y., Yin, X., Chen, X., Chen, L., & Wang, S. (2017). Magnetic solid-phase  
995 extraction using Fe<sub>3</sub>O<sub>4</sub>@ SiO<sub>2</sub> magnetic nanoparticles followed by UV-Vis  
996 spectrometry for determination of paraquat in plasma and urine samples. *Journal of*  
997 *analytical methods in chemistry*, 2017.

998 Shen, Y., Fang, Q., & Chen, B. (2015). Environmental applications of three-dimensional  
999 graphene-based macrostructures: adsorption, transformation, and  
1000 detection. *Environmental Science & Technology*, 49(1), 67-84.

1001 Sherlala, A. I. A., Raman, A. A. A., Bello, M. M., & Asghar, A. (2018). A review of the  
1002 applications of organo-functionalized magnetic graphene oxide nanocomposites for  
1003 heavy metal adsorption. *Chemosphere*, 193, 1004-1017.

1004 Shi, X., Li, N., Wu, D., Hu, N., Sun, J., Zhou, X., ... & Wu, Y. (2018). Magnetic covalent  
1005 organic framework material: synthesis and application as a sorbent for polycyclic  
1006 aromatic hydrocarbons. *Analytical Methods*, 10(41), 5014-5024.

1007 Shi, Y., Hu, K., Cui, Y., Cheng, J., Zhao, W., & Li, X. (2019). Magnetic triptycene-based  
1008 covalent triazine frameworks for the efficient extraction of anthraquinones in slimming  
1009 tea followed by UHPLC-FLD detection. *Microchemical Journal*, 146, 525-533.

1010 Sobhi, H. R., Ghambarian, M., Behbahani, M., & Esrafil, A. (2017). Application of  
1011 dispersive solid phase extraction based on a surfactant-coated titanium-based

1012 nanomagnetic sorbent for preconcentration of bisphenol A in water samples. *Journal*  
1013 *of Chromatography A*, 1518, 25-33.

1014 Speltini, A., Sturini, M., Maraschi, F., & Profumo, A. (2016). Recent trends in the  
1015 application of the newest carbonaceous materials for magnetic solid-phase extraction  
1016 of environmental pollutants. *Trends in Environmental Analytical Chemistry*, 10, 11-  
1017 23.

1018 Su, H., Lin, Y., Wang, Z., Wong, Y. L. E., Chen, X., & Chan, T. W. D. (2016). Magnetic  
1019 metal–organic framework–titanium dioxide nanocomposite as adsorbent in the  
1020 magnetic solid-phase extraction of fungicides from environmental water  
1021 samples. *Journal of Chromatography A*, 1466, 21-28.

1022 Su, H., Li, W., Han, Y., & Liu, N. (2018). Magnetic carboxyl functional nanoporous  
1023 polymer: synthesis, characterization and its application for methylene blue  
1024 adsorption. *Scientific reports*, 8(1), 1-8.

1025 Tahmasebi, E., Yamini, Y., Seidi, S., & Rezazadeh, M. (2013). Extraction of three  
1026 nitrophenols using polypyrrole-coated magnetic nanoparticles based on anion  
1027 exchange process. *Journal of Chromatography A*, 1314, 15-23.

1028 Tolessa, T., Zhou, X. X., Amde, M., & Liu, J. F. (2017). Development of reusable magnetic  
1029 chitosan microspheres adsorbent for selective extraction of trace level silver  
1030 nanoparticles in environmental waters prior to ICP-MS analysis. *Talanta*, 169, 91-97.

1031 Uribe-Romo, F. J., Hunt, J. R., Furukawa, H., Klock, C., O’Keeffe, M., & Yaghi, O. M.  
1032 (2009). A crystalline imine-linked 3-D porous covalent organic framework. *Journal of*  
1033 *the American Chemical Society*, 131(13), 4570-4571.

1034 Uribe-Romo, F. J., Doonan, C. J., Furukawa, H., Oisaki, K., & Yaghi, O. M. (2011).  
1035 Crystalline covalent organic frameworks with hydrazone linkages. *Journal of the*  
1036 *American Chemical Society*, 133(30), 11478-11481.

1037 Waller, P. J., Lyle, S. J., Osborn Popp, T. M., Diercks, C. S., Reimer, J. A., & Yaghi, O.  
1038 M. (2016). Chemical conversion of linkages in covalent organic frameworks. *Journal*  
1039 *of the American Chemical Society*, 138(48), 15519-15522.

1040 Wan H, Huang J, Liu Z, Li J, Zhang W, Zou H. A. (2015). dendrimer-assisted magnetic  
1041 graphene-silica hydrophilic composite for efficient and selective enrichment of  
1042 glycopeptides from the complex sample. *Chem Commun (Camb)*, 7;51(45), 9391-4.

1043 Wan, T., Li, W., & Chen, Z. (2021). Metal organic framework-801 based magnetic solid-  
1044 phase extraction and its application in analysis of preterm labor treatment  
1045 drugs. *Journal of Pharmaceutical and Biomedical Analysis*, 114049.

1046 Wang, J., Li, J., Yan, G., Gao, M., Zhang, X, (2019). Preparation of thickness-controlled  
1047 Mg-MOFs based magnetic graphene composite as a novel hydrophilic matrix for the  
1048 effective identification of glycopeptide in human urine. *Nanoscale*, **11**, 3701-3709.

1049 Wang, J., & Qiu, J. (2016). A review of carbon dots in biological applications. *Journal of*  
1050 *materials science*, 51(10), 4728-4738.

1051 Wang, M., Yang, X., & Bi, W. (2015a). Application of magnetic graphitic carbon nitride  
1052 nanocomposites for the solid-phase extraction of phthalate esters in water  
1053 samples. *Journal of separation science*, 38(3), 445-452.

1054 Wang, M., Cui, S., Yang, X., & Bi, W. (2015b). Synthesis of g-C<sub>3</sub>N<sub>4</sub>/Fe<sub>3</sub>O<sub>4</sub>  
1055 nanocomposites and application as a new sorbent for solid phase extraction of  
1056 polycyclic aromatic hydrocarbons in water samples. *Talanta*, 132, 922-928.

1057 Wang, R., & Chen, Z. (2017a). A covalent organic framework-based magnetic sorbent for  
1058 solid phase extraction of polycyclic aromatic hydrocarbons, and its hyphenation to  
1059 HPLC for quantitation. *Microchimica Acta*, 184(10), 3867-3874.

1060 Wang, H., Jiao, F., Gao, F., Huang, J., Zhao, Y., Shen, Y., ... & Qian, X. (2017b). Facile  
1061 synthesis of magnetic covalent organic frameworks for the hydrophilic enrichment of  
1062 N-glycopeptides. *Journal of Materials Chemistry B*, 5(22), 4052-4059.

1063 Wang, X., Ma, X., Huang, P., Wang, J., Du, T., Du, X., & Lu, X. (2018b). Magnetic Cu-  
1064 MOFs embedded within graphene oxide nanocomposites for enhanced  
1065 preconcentration of benzenoid-containing insecticides. *Talanta*, 181, 112-117.

1066 Wang, Y., Xie, J., Wu, Y., & Hu, X. (2014). A magnetic metal-organic framework as a new  
1067 sorbent for solid-phase extraction of copper (II), and its determination by  
1068 electrothermal AAS. *Microchimica Acta*, 181(9-10), 949-956.

1069 Wang, Z., Zhang, X., Jiang, S., & Guo, X. (2018a). Magnetic solid-phase extraction based  
1070 on magnetic multiwalled carbon nanotubes for the simultaneous enantiomeric  
1071 analysis of five  $\beta$ -blockers in the environmental samples by chiral liquid  
1072 chromatography coupled with tandem mass spectrometry. *Talanta*, 180, 98-107.

1073 Wei, P. F., Qi, M. Z., Wang, Z. P., Ding, S. Y., Yu, W., Liu, Q., ... & Wang, W. (2018).  
1074 Benzoxazole-linked ultrastable covalent organic frameworks for  
1075 photocatalysis. *Journal of the American Chemical Society*, 140(13), 4623-4631.

1076 Wen, Y., Zhang, P., Sharma, V. K., Ma, X., & Zhou, H. C. (2021). Metal-organic  
1077 frameworks for environmental applications. *Cell Reports Physical Science*, 100348.

1078 Wu, R., Ma, F., Zhang, L., Li, P., Li, G., Zhang, Q., ... & Wang, X. (2016). Simultaneous  
1079 determination of phenolic compounds in sesame oil using LC-MS/MS combined with  
1080 magnetic carboxylated multi-walled carbon nanotubes. *Food chemistry*, 204, 334-  
1081 342.

1082 Wu, Y., Sun, N., Deng, C. (2020). Construction of Magnetic Covalent Organic  
1083 Frameworks with Inherent Hydrophilicity for Efficiently Enriching Endogenous  
1084 Glycopeptides in Human Saliva. *ACS Applied. Material. Interfaces*, 12, 9814-9823

1085 Xiang, G., Ma, Y., Jiang, X., & Mao, P. (2014). Polyelectrolyte multilayers on magnetic  
1086 silica as a new sorbent for the separation of trace copper in food samples and  
1087 determination by flame atomic absorption spectrometry. *Talanta*, 130, 192-197.

1088 Yang, P., Gai, S., & Lin, J. (2012). Functionalized mesoporous silica materials for  
1089 controlled drug delivery. *Chemical Society Reviews*, 41(9), 3679-3698.

1090 Yang, X. A., Shi, M. T., Leng, D., & Zhang, W. B. (2018). Fabrication of a porous  
1091 hydrangea-like Fe<sub>3</sub>O<sub>4</sub>@ MnO<sub>2</sub> composite for ultra-trace arsenic preconcentration  
1092 and determination. *Talanta*, 189, 55-64.

1093 Yang, Y., Ali, F., Said, A., Ali, N., Ahmad, S., Raziq, F., & Khan, S. (2021a). Fabrication,  
1094 mechanical, and electromagnetic studies of cobalt ferrite based-epoxy  
1095 nanocomposites. *Polymer Composites*, 42(1), 285-296.

1096 Yang, Y., Ali, N., Khan, A., Khan, S., Khan, S., Khan, H., ... & Bilal, M. (2021b). Chitosan-  
1097 capped ternary metal selenide nanocatalysts for efficient degradation of Congo red  
1098 dye in sunlight irradiation. *International Journal of Biological Macromolecules*, 167,  
1099 169-181.

1100 Yang, J., Qiao, J. Q., Cui, S. H., Li, J. Y., Zhu, J. J., Yin, H. X., ... & Lian, H. Z. (2015).  
1101 Magnetic solid-phase extraction of brominated flame retardants from environmental  
1102 waters with graphene-doped Fe<sub>3</sub>O<sub>4</sub> nanocomposites. *Journal of separation  
1103 science*, 38(11), 1969-1976.

1104 Yu, J., Zhu, S., Pang, L., Chen, P., & Zhu, G. T. (2018). Porphyrin-based magnetic  
1105 nanocomposites for efficient extraction of polycyclic aromatic hydrocarbons from  
1106 water samples. *Journal of Chromatography A*, 1540, 1-10.

1107 Yu, M., Wang, L., Hu, L., Li, Y., Luo, D., & Mei, S. (2019). Recent applications of magnetic  
1108 composites as extraction adsorbents for determination of environmental  
1109 pollutants. *TrAC Trends in Analytical Chemistry*, 119, 115611.

1110 Zahn, G., Zerner, P., Lippke, J., Kempf, F. L., Lilienthal, S., Schröder, C. A., ... & Behrens,  
1111 P. (2014). Insight into the mechanism of modulated syntheses: in situ synchrotron  
1112 diffraction studies on the formation of Zr-fumarate MOF. *CrystEngComm*, 16(39),  
1113 9198-9207.

1114 Zaman, H., Ali, N., Gao, X., Zhang, S., Hong, K., & Bilal, M. (2019). Effect of pH and  
1115 salinity on stability and dynamic properties of magnetic composite amphiphilic  
1116 demulsifier molecules at the oil-water interface. *Journal of Molecular Liquids*, 290,  
1117 111186.

1118 Zeb, S., Ali, N., Ali, Z., Bilal, M., Adalat, B., Hussain, S., ... & Iqbal, H. M. (2020). Silica-  
1119 based nanomaterials as designer adsorbents to mitigate emerging organic  
1120 contaminants from water matrices. *Journal of Water Process Engineering*, 38,  
1121 101675.

1122 Zhang, B., Wei, M., Mao, H., Pei, X., Alshimri, S. A., Reimer, J. A., & Yaghi, O. M.  
1123 (2018). Crystalline dioxin-linked covalent organic frameworks from irreversible  
1124 reactions. *Journal of the American Chemical Society*, 140(40), 12715-12719.

1125 Zhang, Q., Huang, Y., Jiang, B., Hu, Y., Xie, J., Gao, X., Jia, B., Shen, H., Zhang, W.,  
1126 and Yang, P. (2018). In Situ Synthesis of Magnetic Mesoporous Phenolic Resin for  
1127 the Selective Enrichment of Glycopeptides. *Analytical Chemistry*, 90 (12), 7357-7363

1128 Zhan, Q., Zhao, H., Hong, Y., Pu, C., Liu, Y., & Lan, M. (2019). Preparation of a  
1129 hydrophilic interaction liquid chromatography material by sequential electrostatic  
1130 deposition of layers of polyethyleneimine and hyaluronic acid for enrichment of  
1131 glycopeptides. *Microchimica Acta*, 186(9), 1-10.

1132 Zhang, B., Li, P., Zhang, H., Li, X., Tian, L., Wang, H., ... & Zhang, Q. (2016a). Red-blood-  
1133 cell-like BSA/Zn<sub>3</sub> (PO<sub>4</sub>)<sub>2</sub> hybrid particles: Preparation and application to adsorption  
1134 of heavy metal ions. *Applied Surface Science*, 366, 328-338.

1135 Zhang, B., Zhang, H., Tian, L., Li, X., Li, W., Fan, X., ... & Zhang, Q. (2015). Magnetic  
1136 microcapsules with inner asymmetric structure: Controlled preparation, mechanism,  
1137 and application to drug release. *Chemical Engineering Journal*, 275, 235-244.

1138 Zhang, B., Zhang, H., Zhou, L., Ali, N., Geng, W., & Zhang, Q. (2013). PREPARATION  
1139 OF FLOWER-LIKE  $\text{Co}_3\text{O}_4/\text{Fe}_3\text{O}_4$  MAGNETIC MICROSPHERES FOR  
1140 PHOTODEGRADATION OF RhB UNDER UV LIGHT. *Functional Materials*  
1141 *Letters*, 6(06), 1350052.

1142 Zhang, H., Lv, Y., Du, J., Shao, W., Jiao, F., Xia, C., ... & Qian, X. (2020b). A GSH  
1143 Functionalized Magnetic Ultra-thin 2D-MoS<sub>2</sub> nanocomposite for HILIC-based  
1144 enrichment of N-glycopeptides from urine exosome and serum proteins. *Analytica*  
1145 *chimica acta*, 1098, 181-189.

1146 Zhang, H., Zheng, D., Zhou, Y., Xia, H., & Peng, X. (2020a). Multifunctionalized magnetic  
1147 mesoporous silica as an efficient mixed-mode sorbent for extraction of phenoxy  
1148 carboxylic acid herbicides from water samples followed by liquid chromatography-  
1149 mass spectrometry in tandem. *Journal of Chromatography A*, 1634, 461645.

1150 Zhang, L., Yue, X., Li, N., Shi, H., Zhang, J., Zhang, Z., & Dang, F. (2019a). One-step  
1151 maltose-functionalization of magnetic nanoparticles based on self-assembled  
1152 oligopeptides for selective enrichment of glycopeptides. *Analytica chimica*  
1153 *acta*, 1088, 63-71.

1154 Zhang, M., Li, J., Zhang, C., Wu, Z., Yang, Y., Li, J., ... & Lin, Z. (2020c). In-situ synthesis  
1155 of fluorinated magnetic covalent organic frameworks for fluorinated magnetic solid-  
1156 phase extraction of ultratrace perfluorinated compounds from milk. *Journal of*  
1157 *Chromatography A*, 1615, 460773.

1158 Zhang, S., Jiao, Z., & Yao, W. (2014). A simple solvothermal process for fabrication of a  
1159 metal-organic framework with an iron oxide enclosure for the determination of  
1160 organophosphorus pesticides in biological samples. *Journal of Chromatography*  
1161 *A*, 1371, 74-81.

1162 Zhang, S., Yao, W., Ying, J., & Zhao, H. (2016b). Polydopamine-reinforced magnetization  
1163 of zeolitic imidazolate framework ZIF-7 for magnetic solid-phase extraction of  
1164 polycyclic aromatic hydrocarbons from the air-water environment. *Journal of*  
1165 *Chromatography A*, 1452, 18-26.

1166 Zhang, W., Liang, F., Li, C., Qiu, L. G., Yuan, Y. P., Peng, F. M., ... & Zhu, J. F. (2011).  
1167 Microwave-enhanced synthesis of magnetic porous covalent triazine-based  
1168 framework composites for fast separation of organic dye from aqueous  
1169 solution. *Journal of hazardous materials*, 186(2-3), 984-990.

1170 Zhang, W., Lan, C., Zhang, H., Zhang, Y., Zhang, W., Zhao, W., ... & Zhang, S. (2019b).  
1171 Facile preparation of dual-shell novel covalent–organic framework functionalized  
1172 magnetic nanospheres used for the simultaneous determination of fourteen trace  
1173 heterocyclic aromatic amines in nonsmokers and smokers of cigarettes with different  
1174 tar yields based on UPLC-MS/MS. *Journal of agricultural and food chemistry*, 67(13),  
1175 3733-3743.

1176 Zhang, Y., Zhou, H., Zhang, Z. H., Wu, X. L., Chen, W. G., Zhu, Y., ... & Zhao, Y. G.  
1177 (2017). Three-dimensional ionic liquid functionalized magnetic graphene oxide  
1178 nanocomposite for the magnetic dispersive solid phase extraction of 16 polycyclic  
1179 aromatic hydrocarbons in vegetable oils. *Journal of Chromatography A*, 1489, 29-38.

1180 Zhao, J., Luque, R., Qi, W., Lai, J., Gao, W., Gilani, M. R. H. S., & Xu, G. (2015). Facile  
1181 surfactant-free synthesis and characterization of Fe<sub>3</sub>O<sub>4</sub>@ 3-aminophenol–  
1182 formaldehyde core–shell magnetic microspheres. *Journal of Materials Chemistry*  
1183 *A*, 3(2), 519-524.

1184 Zhao, L., Qin, H., Wu, R. A., & Zou, H. (2012). Recent advances of mesoporous materials  
1185 in sample preparation. *Journal of Chromatography A*, 1228, 193-204.

1186 Zhao, X., Liu, S., Wang, P., Tang, Z., Niu, H., Cai, Y., ... & Giesy, J. P. (2015). Surfactant-  
1187 modified flowerlike layered double hydroxide-coated magnetic nanoparticles for  
1188 preconcentration of phthalate esters from environmental water samples. *Journal of*  
1189 *Chromatography A*, 1414, 22-30.

1190 Zhao, Y., Wang, C., Wang, S., Wang, C., Liu, Y., Al-Khalaf, A. A., ... & Zhao, D. (2018).  
1191 Magnetic mesoporous TiO<sub>2</sub> microspheres for sustainable arsenate removal from  
1192 acidic environments. *Inorganic Chemistry Frontiers*, 5(9), 2132-2139.

1193 Zheng, H., Guan, S., Wang, X., et al. (2020a). Deconstruction of Heterogeneity of Size-  
1194 Dependent Exosome Subpopulations from Human Urine by Profiling N-  
1195 Glycoproteomics and Phosphoproteomics Simultaneously. *Analytical Chemistry*, 92,  
1196 13, 9239–9246

- 1197 Zheng, H., Jia, J., Li, Z., & Jia, Q. (2020b). Bifunctional magnetic supramolecular-organic  
1198 framework: A nanoprobe for simultaneous enrichment of glycosylated and  
1199 phosphorylated peptides. *Analytical chemistry*, 92(3), 2680-2689.
- 1200 Zheng, X., He, L., Duan, Y., Jiang, X., Xiang, G., Zhao, W., & Zhang, S. (2014). Poly  
1201 (ionic liquid) immobilized magnetic nanoparticles as new adsorbent for extraction and  
1202 enrichment of organophosphorus pesticides from tea drinks. *Journal of*  
1203 *Chromatography A*, 1358, 39-45.
- 1204 Zhou, C., Zhang, W., Xia, M., Zhou, W., Wan, Q., Peng, K., & Zou, B. (2013). Synthesis  
1205 of poly (acrylic acid) coated-Fe<sub>3</sub>O<sub>4</sub> superparamagnetic nano-composites and their  
1206 fast removal of dye from aqueous solution. *Journal of nanoscience and*  
1207 *nanotechnology*, 13(7), 4627-4633.
- 1208 Zhou, M., Wang, T., He, Z., Xu, Y., Yu, W., Shi, B., & Huang, K. (2019). Synthesis of yolk-  
1209 shell magnetic porous organic nanospheres for efficient removal of methylene blue  
1210 from water. *ACS Sustainable Chemistry & Engineering*, 7(3), 2924-2932.
- 1211 Zhou, Q., Lei, M., Wu, Y., & Yuan, Y. (2017a). Magnetic solid phase extraction of typical  
1212 polycyclic aromatic hydrocarbons from environmental water samples with metal  
1213 organic framework MIL-101 (Cr) modified zero valent iron nano-particles. *Journal of*  
1214 *Chromatography A*, 1487, 22-29.
- 1215 Zhou, Q., Lei, M., Liu, Y., Wu, Y., & Yuan, Y. (2017b). Simultaneous determination of  
1216 cadmium, lead and mercury ions at trace level by magnetic solid phase extraction  
1217 with Fe@ Ag@ Dimercaptobenzene coupled to high performance liquid  
1218 chromatography. *Talanta*, 175, 194-199.
- 1219 Zhou, Q., Yuan, Y., Sun, Y., Sheng, X., & Tong, Y. (2021). Magnetic solid phase  
1220 extraction of heterocyclic aromatic hydrocarbons from environmental water samples  
1221 with multiwalled carbon nanotube modified magnetic polyamido-amine dendrimers  
1222 prior to gas chromatography-triple quadrupole mass spectrometer. *Journal of*  
1223 *Chromatography A*, 1639, 461921.
- 1224 Zhou, S., Song, N., Lv, X., & Jia, Q. (2018). Preparation of carboxylatocalix [4] arene  
1225 functionalized magnetic polyionic liquid hybrid material for the pre-concentration of  
1226 phthalate esters. *Journal of Chromatography A*, 1565, 19-28.

1227 Zhou, Y., Tao, Y., Li, H., Zhou, T., Jing, T., Zhou, Y., & Mei, S. (2016b). Occurrence  
1228 investigation of perfluorinated compounds in surface water from East Lake (Wuhan,  
1229 China) upon rapid and selective magnetic solid-phase extraction. *Scientific*  
1230 *reports*, 6(1), 1-10.

1231 Zhou, Y., He, Z., Tao, Y., Xiao, Y., Zhou, T., Jing, T., ... & Mei, S. (2016a). Preparation of  
1232 a functional silica membrane coated on Fe<sub>3</sub>O<sub>4</sub> nanoparticle for rapid and selective  
1233 removal of perfluorinated compounds from surface water sample. *Chemical*  
1234 *Engineering Journal*, 303, 156-166.

1235 Zhu, G. T., Li, X. S., Gao, Q., Zhao, N. W., Yuan, B. F., & Feng, Y. Q. (2012).  
1236 Pseudomorphic synthesis of monodisperse magnetic mesoporous silica  
1237 microspheres for selective enrichment of endogenous peptides. *Journal of*  
1238 *Chromatography A*, 1224, 11-18.

1239  
1240  
1241  
1242  
1243  
1244  
1245  
1246  
1247  
1248  
1249  
1250  
1251  
1252  
1253  
1254  
1255  
1256  
1257

1258 **List of Tables**1259 **Table 1** Summary of some magnetic carbon based solid-phase extraction sorbent materials

Adsorbent	Sample	Pollutant	Adsorption (mg g <sup>-1</sup> )	Separation technique	Recoveries (%)	References
G/Fe <sub>3</sub> O <sub>4</sub> @PT	Water	PAHs		GC-FID	83-107	(Mehdinia et al., 2015)
GOePAR@Fe <sub>3</sub> O <sub>4</sub>	Food, water	Pb(II)	133	ETAAS	94.3-107	(Akbarzade et al., 2018)
GO-Fe <sub>3</sub> O <sub>4</sub> @PS	Water	PAHs		GC-FID	95.8-99.5	(Amiri et al., 2018)
Fe <sub>3</sub> O <sub>4</sub> @MWCNTs	Water, human urine	Parabens		GC-MS	81-119	(Pastorbelda et al., 2018)
Mag-MMWCNTs	Environmental water	β-blockers		Chiral UPLC-MS/MS	82.9-95.6	(Wang et al., 2018)
c-MWCNT-MNPs	Sesame oil	Herbicides phenolic		HPLC-MS/MS	83.8-125.9	(Wu et al., 2016)
m-G/CNF	Environmental water	PAHs		GC-FID	95.5-99.9	(Rezvani-Eivari et al., 2016)
g-C <sub>3</sub> N <sub>4</sub> /Fe <sub>3</sub> O <sub>4</sub>	Water	PAEs	4.14-18.02	HPLC-UV	79.4-99.4	(Wang et al., 2015a)
g-C <sub>3</sub> N <sub>4</sub> /Fe <sub>3</sub> O <sub>4</sub>	Water	PAHs		HPLC-UV	80.0-99.8	(Wang, M et al., 2015b)

1260

1261

1262

1263

1264

1265

1266

1267

1268

1269

1270

1271

1272

1273

1274

1275

1276

1277 **Table 2** Summary of some MOF based magnetic solid-phase extraction sorbent materials

Adsorbent	Sample	Pollutant	Adsorption (mg g <sup>-1</sup> )	Separation technique	Recoveries (%)	References
Fe <sub>3</sub> O <sub>4</sub> eNH <sub>2</sub> @MIL-101(Cr)	Water	Pyrethroids		GC-ECD	72.1-106.8	(He et al., 2018)
Fe@MIL101(Cr)	River water	PAHs		HPLC-VWD	85.7-97.3	(Zhou et al., 2017a)
Fe <sub>3</sub> O <sub>4</sub> @SiO <sub>2</sub> -MIL-101(Cr)	Water	Pesticides		HPLC-DAD	80.2-107.5	(Ma et al., 2016a)
Fe <sub>3</sub> O <sub>4</sub> @MIL-101(Fe)	Human hair, urine	OPPs		GC-FPD	74.9-94.5	(Zhang et al., 2014)
magnetic MIL-100(Fe)	Environmental water	PAHs		GC-FID	88.5-106.6	(Hou et al., 2017)
MAA@Fe <sub>3</sub> O <sub>4</sub> -ZIF-8	Water	PAEs		HPLC-DAD	85.6-103.6	(Liu et al., 2015)
Fe <sub>3</sub> O <sub>4</sub> @PDA@ZIF-7	Rainwater, PM2.5	PAHs		GC-MS	82.1-99.4	(Zhang et al., 2016b)
PSA@Zr-MOF@Fe <sub>3</sub> O <sub>4</sub>	Environmental	Herbicides		UPLC-HRMS	86.2-104.6	(Pan et al., 2019)
Fe <sub>3</sub> O <sub>4</sub> @HKUST-1	Water, fruit-tea	PAHs		UPLC-FLD	75-94	(Rocio-Bautista et al., 2016)
Magnetic MOF-5	River water	heterocyclic	81-181	HPLC-FLD	80.20-108.33	(Ma et al., 2018)
Fe <sub>3</sub> O <sub>4</sub> @DMcT@HKUST-1	Baby food	Cd(II), Zn(II), Pb(II)	155-190	FAAS	90.0-106	(Ghorbani et al., 2015)
Fe <sub>3</sub> O <sub>4</sub> @IRMOF-3	Water	Cu(II)	2.4	ETAAS	98.0-102.0	(Wang et al., 2014)
COF-LZU1@PEI@Fe <sub>3</sub> O <sub>4</sub>	Water, soil	PAHs		HPLC-FLD	85.1-107.8	(Wang R et al., 2017a)

1278

1279

1280

1281

1282

1283

1284

1285

1286

1287

1288

1289

1290

1291

1292

1293 **Table 3.** Representative magnetic MOFs as adsorbents for glycoproteins and glycopeptides.

Magnetic MOFs material	Samples	Selectivity	Sensitivity	Identified glycopeptides	Reference
L-Cys-Fe <sub>3</sub> O <sub>4</sub> @mSiO <sub>2</sub>	Human saliva (healthy volunteer; gastric cancer volunteer)	HRP:BSA = 1:100 (mass ratio)	1 fmol/μL HRP digest	46; 36	(Chen et al., 2019a)
MagG@PEI@HA	Human serum	HRP:BSA = 1:1000 (molar ratio)	2 fmol/μL IgG digest	376	(Zhan et al., 2019)
Fe <sub>3</sub> O <sub>4</sub> -GO@PDA-Chitosan	Human renal mesangial cells	HRP:BSA = 1:10 (molar ratio)	0.4 fmol/μL HRP digest	393	(Changfen et al., 2020)
SPIOs@SiO <sub>2</sub> @MOF	Mouse liver	IgG:BSA = 1:500 (mass ratio)	10 fmol/μL IgG digest	152	(Luo et al., 2019)
MoS <sub>2</sub> -Fe <sub>3</sub> O <sub>4</sub> -Au/NWs-GSH	Human urine exosome; serum	IgG:BSA = 1:1000 (mass ratio)	0.5 fmol/μL IgG digest	1250; 489	(Zhang et al., 2020b)
Fe <sub>3</sub> O <sub>4</sub> -PEI-pMaltose	Human renal mesangial cells	HRP:BSA = 1:100 (mass ratio)	10 fmol/μL HRP digest	449	(Qi et al., 2021)
Fe <sub>3</sub> O <sub>4</sub> @TpPa-1	Human serum	IgG:BSA = 1:100 (molar ratio)	28 fmol/μL IgG digest	228	(Wang et al., 2017b)
AEK8-maltose functionalized SiO <sub>2</sub> @Fe <sub>3</sub> O <sub>4</sub>	Human serum	HRP:BSA = 1:150 (mass ratio)	0.001 ng/μL HRP digest	282	(Zhang et al., 2019a)
MCNCs@COF@PBA	Exosomes secreted from the	HRP:BSA = 1:600 (mass ratio)	100 amol/μL HRP digest	32	(Gao et al., 2019)
magOTfP5SOF-Ga <sup>3+</sup>	Hela cell human lung adenocarcinoma cells; mouse liver tissue	HRP:BSA = 1:2000 (mass ratio)	0.1 fmol/μL HRP digest	147	(Zheng et al 2020a)
MMP	Human serum	HRP digest:BSA protein = 1:50 (mass ratio)	–	365	(Zhang et al., 2018)
Fe <sub>3</sub> O <sub>4</sub> -GO@nSiO <sub>2</sub> -PAMAM	Mouse liver	–	0.5 fmol/μL IgG digest	1529	(Wan et al 2015)
CFMZOF	Exosomes from human urine	HRP:BSA = 1:100 (mass ratio)	0.5 fmol/μL HRP digest	335; 375; 389	(Zheng et al., 2020b)
mCTpBD	Human saliva (healthy people; patients with inflammatory bowel disease)	HRP digest:BSA protein = 1:1000 (mass ratio)	0.5 fmol/μL HRP digest	32; 39	(Wu et al., 2020)
MagG@Mg-MOFs-1C	Human urine	HRP digest:BSA	0.1 fmol/μL HRP digest	406	(Wang et al 2019)

		protein = 1:500 (mass ratio)			
	magHN/Au-GSH nanofiber	Human serum	IgG:BSA = 1:500 (molar ratio)	2 fmol/ $\mu$ L IgG digest	246 (Huan et al., 2019)
1294					
1295					
1296					
1297					
1298					
1299					
1300					
1301					
1302					
1303					
1304					
1305					
1306					
1307					
1308					
1309					
1310					
1311					
1312					
1313					
1314					
1315					
1316					
1317					
1318					
1319					
1320					
1321					
1322					
1323					
1324					
1325					
1326					

1327 **Table 4** Data explaining the application of MNPs-COFs for removal of metals, dyes and others.

Magnetic porous organic framework (M-POFs)	Medium	Pollutant	Pore size (nm)	Analytical Techniques	Adsorption (mg.g <sup>-1</sup> )	References
Magnetic porous organic polymers MOP	Water	Methylene blue » Methylene Orange	e	Uv-visible	1153	(Huang et al., 2017)
Tannin-based magnetic porous organic polymers (TA-MOPs)	Water	Methylene blue/Pb	9.6	inductively coupled plasma optical emission spectrometer and Uv-Vis	1326 to 1727	(Huang et al., 2019)
Magnetic carboxyl functional nanoporous polymer	Water	Methylene blue	20 to 40	Uv-visible	57.74	(Su et al., 2018)
Magnetic triazine-based covalent framework (CTF/Fe <sub>2</sub> O <sub>3</sub> )	Water	Methylene Orange	21 to 40	UV-visible	291	(Zhang et al., 2011)
Fe <sub>3</sub> O <sub>4</sub> @3-aminophenol-formaldehyde	Water	Methylene blue	e	e	e	(Zhao et al., 2015)
Fe <sub>3</sub> O <sub>4</sub> /Hypercrosslinked polymers	Water	Methylene Orange and fuchsin basic	0.73 and 1.36	UV-visible	211 to 231	(Pan et al., 2016)
Yolk-shell magnetic porous organic nanoparticles	Water	Methylene blue	e	Uv-visible	134	(Zhou et al., 2019)
Magnetic β-cyclodextrin (β-CD) porous polymer nanospheres (P-MCD)	Water	Methylene blue	5.59	UV-visible	305.8	(Liu et al., 2019)
Copper ferrite-polyaniline nanocomposite CuFe/PANI	Water	Methylene Orange	-	UV-visible	345.9	(Kharazi et al., 2019)
Triazine-based polymeric network/MNPs	Water	Methylene Orange	-	UV-visible	80.6	(Faraji et al., 2018)
poly(acrylic acid)/Fe <sub>3</sub> O <sub>4</sub>	Water	methylene blue	-	Uv-visible	73.85	(Zhou et al., 2013)
Sodium acrylate (SA)/Fe <sub>3</sub> O <sub>4</sub> nanoparticles (SA-MMNPs)	Water	Rhodamine B	-	e	216	(Li et al., 2017b)
Magnetic 1,3,5-triphenylbenzene-benzidine (Fe <sub>3</sub> O <sub>4</sub> /TpBD)	Water	Bisphenols	-	UV-visible	160.6 to 236.7	(Li Y et al., 2017c)
Magnetic hyper-cross-linked polymers	e	Antibiotics	-	UV-visible	114.94 to 212.7	(Liu Y et al., 2018b)

---

Fe<sub>3</sub>O<sub>4</sub>/COF-LZU-1

Water

Iodine

1.1 to 1.3

UV-visible

797

(Liao et al., 2017)

---

1328

1329

1330

1331

1332

1333

1334

1335

1336

1337

1338

1339

1340

1341

1342

1343

1344

1345

1346

1347

1348

1349

1350

1351

1352

1353

1354

1355

1356

1357

1358

1359

1360

1361

1362

1363

1364 **Table 5** Preparation and application of M-POFs in the determination of heavy metal and other emerging  
 1365 organic contaminants.

M-POFs	Matrix	Pollutant	SBET (m <sup>2</sup> g <sup>-1</sup> )	Analytical instruments	Recovery (%)	References
Magnetic TpPa-1	Water	PAHs	-----	HPLC-FLD	73 to 110	(He et al., 2017a)
Fe <sub>3</sub> O <sub>4</sub> /TpBD	Grilled fish, wild fish,	PAHs	248	HPLC-DAD	84.3 to 104.3	(Li et al., 2018)
COF-LZU1-PEI/Fe <sub>3</sub> O <sub>4</sub>	Soil, water and coffee	PAHs	115	HPLC-UV/FLD	85.1 to 105	(Wang et al., 2017)
Fe <sub>3</sub> O <sub>4</sub> /COF(TpDA)	Edible oil, grilled fish and chicken	PAHs	-----	HPLC-DAD	85.7 to 104.2	(Shi et al., 2018)
Fe <sub>3</sub> O <sub>4</sub> /SiO <sub>2</sub> -TCPP	Water	PAHs	-----	GC-MS	71.1 to 106.0	(Yu et al., 2018)
Fe <sub>3</sub> O <sub>4</sub> /SiO <sub>2</sub> @PAF-6	Cigarette smoke and water	Phenols,	-----	HPLC-UV/FLD	84.0 to 94.0	(Chen et al., 2018)
TpBD-DS MNS	Urine	PAHs,	180	UPLC-MS/MS	95.4 to 129.3	(Zhang et al., 2019b)
CTC-COF-MCNT	Fried chicken, roast beef	HAAs	-----	UPLC-MS/MS	73.0 to 117	(Liang et al., 2020)
CTF/Fe <sub>2</sub> O <sub>3</sub>	Water	PFCs	-----	HPLC	81.9e114	(Ren et al., 2018)
Fe <sub>3</sub> O <sub>4</sub> /TpPa-F4	Milk	PFCs	120	HPLC-MS/MS	73.27 to 128.07	(Zhang M et al., 2020c)
Fe <sub>3</sub> O <sub>4</sub> /COF(TpDA)	Fruits, vegetables	PGRs	-----	HPLC-DAD	83.0 to 105.0	(Li M et al., 2020)
Fe <sub>3</sub> O <sub>4</sub> /COF-(NO <sub>2</sub> ) <sub>2</sub>	Vegetables	Neonicotinoids	171	HPLC	77.5 to 110.2	(Lu et al., 2020)
Ni-POFs	Urine	Alkaloids	429	UHPLC-MS/MS	93.5 to 99.2	(Hu et al., 2020)
M-CTF-TPC	Slimming tea	Anthraquinone		MS UHPLC-FLD	94.5 to 105.4	(Shi et al., 2019)
Fe <sub>3</sub> O <sub>4</sub> /PPy	Water	Nitrophenols	-----	HPLC-UV	84 to 109	(Tahmasebi et al., 2013)
Fe <sub>3</sub> O <sub>4</sub> /SiO <sub>2</sub> GMA-S-SH	Farmland water,	MeHg <sup>b</sup>	188	ICP-MS	84.3 to 116	(He et al., 2019)
g-Fe <sub>2</sub> O <sub>3</sub> /CTF-1	Water, soil and rice samples	PhHg <sup>b</sup>	255	ICP-MS	-----	(Leus et al., 2018)
MOP	Urine, cell	Pt <sup>4b</sup> , Au <sup>3b</sup>	-----	ICP-MS	86 to 110	(Chen et al., 2019b)
Fe <sub>3</sub> O <sub>4</sub> /PANI	Seawater	Bi <sup>3b</sup> MeHg <sup>b</sup>	293	GC-MS	98 to 105	(Mehdinia et al., 2011)

1366

1367

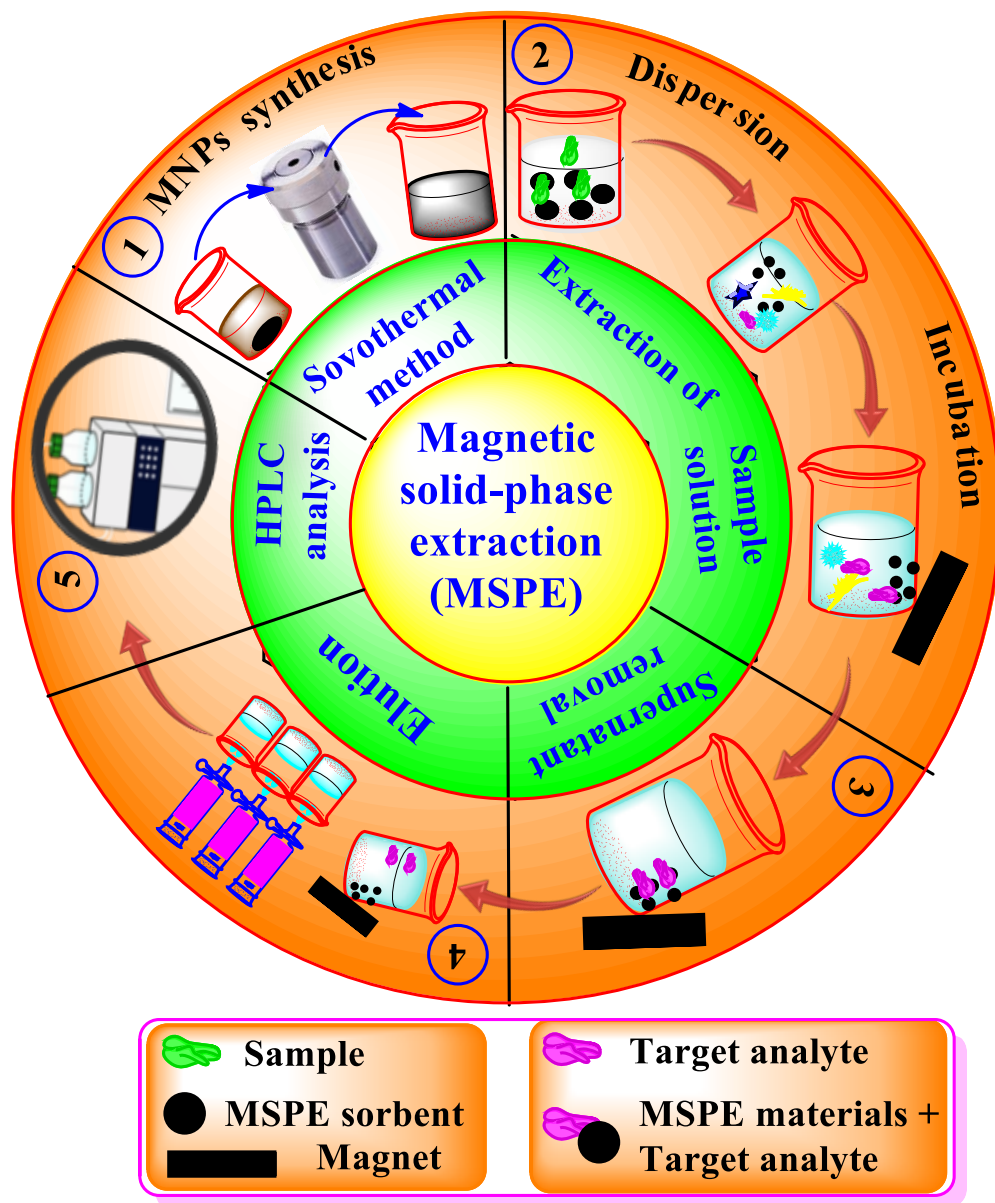
1368

1369 **Table 6** Miscellaneous magnetic nanomaterials for magnetic solid-phase adsorption

Magnetic adsorbents	Samples	Pollutant	Adsorption (mg g <sup>-1</sup> )	Detection techniques	Recovery (%)	Reference
GO-Chm	water, rice	herbicides	29.41 to 35.71	HPLC-UV	94.33 to 102.67	(Shah et al., 2018)
Fe <sub>3</sub> O <sub>4</sub> @SiO <sub>2</sub>	Urine	paraquat	2.4	UveVis	92.9 to 105.2	(Sha et al., 2017)
polythiophene@CS@MNPs	water	triazines	-----	GC-FID	96 to 102	( Feizbakhsh et al., 2016)
Fe <sub>3</sub> O <sub>4</sub> @SiO <sub>2</sub> @MgeAl LDH	water	PAEs	-----	HPLC-UV	63 to 102	(Zhao et al., 2015)
Fe <sub>3</sub> O <sub>4</sub> @Au@2-ME	water	Cd(II),Pb(II), Hg(II)	-----	HPLC-VWD	97.5 to 103.2	(Zhou et al., 2017b)
Fe <sub>3</sub> O <sub>4</sub> @SiO <sub>2</sub> eNH <sub>2</sub> &F <sub>13</sub>	environmental water	PFCs	-----	UPLC-MS/MS	90.05 to 106.67	(Zhou et al., 2016b)
MCM	water	silver nanoparticles	-----	ICP-MS	84.9 to 98.5	(Tolessa et al., 2017)
Fe <sub>3</sub> O <sub>4</sub> @SiO <sub>2</sub> @(PSS-PIL) <sub>n</sub>	water	pesticide	-----	HPLC-UV	82.5 to 109.3	(He et al., 2017b)
Fe <sub>3</sub> O <sub>4</sub> @Au@DDT	water	diphenols, PAHs	-----	HPLC-UV	63.8 to 110.7	(Li et al., 2014)
Fe <sub>3</sub> O <sub>4</sub> @DC193C	water	parabens	-----	HPLC-UV	86.0 to 118.0	(Ariffin et al., 2019)
3D-IL@mGO	vegetable oil	PAHs	7 <sup>e</sup>	GC-MS	80.2 to 115	(Zhang et al., 2017)
Fe <sub>3</sub> O <sub>4</sub> @SiO <sub>2</sub> eC16	water	PCBs	-----	GC-MS/MS	75.17 to 101.20	(Fan et al., 2017)
Fe <sub>3</sub> O <sub>4</sub> @MnO <sub>2</sub>	water	As(III), As(V)	-----	CHG-AFS	85.6 to 111.7	(Yang et al., 2018)
Fe <sub>3</sub> O <sub>4</sub> @SiO <sub>2</sub> @GO@ILs	water	CPs	-----	HPLC-MS/MS	85.3 to 99.3	(Cai et al., 2016)
Fe <sub>3</sub> O <sub>4</sub> @SiO <sub>2</sub> @TiO <sub>2</sub> @CPC	water	BPA	-----	HPLC-UV	92e105	(Sobhi et al., 2017)
MPIL@CC[4]A	water,	PAEs	52.90 to 63.7	HPLC-UV	84.3 to 110.8	(Zhou S.et al., 2018)
PIL-MNPs	tea	OPPs	-----	HPLC-UV	81.4 to 112.6	(Zheng et al., 2014)
SDS@ Fe <sub>3</sub> O <sub>4</sub>	food	cationic dyes	47.4 to 270.3	HPLC-DAD	70.1 to 104.5	(Qi et al., 2016)
Fe <sub>3</sub> O <sub>4</sub> eNH <sub>2</sub> @MIL-101(Cr)	Water	Pyrethroids	72.1-106.8	GC-ECD		(He et al., 2018)
Fe <sub>3</sub> O <sub>4</sub> @PEI-RGO	Rice	Polar acidic	76.34	HPLC-DAD	87.41-102.52	(Li et al., 2017a)
Fe <sub>3</sub> O <sub>4</sub> @G-TEOS-MTMOS	Water	OPPs	37.18	GC-mECD	83-105	(Nodeh et al., 2017)
GOPA@Fe <sub>3</sub> O <sub>4</sub>	Vegetable oil	Herbicides PAHs		HPLC-DAD	85.6-102	(Ji et al., 2017)

PPy-RGOx-Fe <sub>3</sub> O <sub>4</sub>	Bottled water, beverages	PAEs		GC-MS/MS	87.5-99.1	(Pinsrithong et al., 2018)
Fe <sub>3</sub> O <sub>4</sub> @mSiO <sub>2</sub> -Ph-PTSA	Soil	PAHs		GC-MS	86.85-110.01	(Qin et al., 2018)
Fe <sub>3</sub> O <sub>4</sub> @Cr(VI) IIPs	Water	Cr(VI)	2.50	FAAS	98.0-99.2	(Qi et al., 2017)
Fe <sub>3</sub> O <sub>4</sub> @mSiO <sub>2</sub> -eNH <sub>2</sub>	Water, food seafood	highly chlorinated		GC-MS	88.4-103.2	(Liu et al., 2016)
Fe <sub>3</sub> O <sub>4</sub> @mSiO <sub>2</sub> -Me-PTSA	Water	PCBs	46.3	GC-ECD	85.25-118.60	(Qin et al., 2018)
PEMs/Fe <sub>3</sub> O <sub>4</sub> @SiO <sub>2</sub>	Water, rice	Cu(II)	14.7	FAAS	94.4-114.1	(Xiang et al., 2014)
Fe <sub>3</sub> O <sub>4</sub> @SiO <sub>2</sub> @g-MPTS	Water, human hair	Hg(II), MeHg(I)		ICP-MS	75.6-99.6	(Ma et al., 2016b)
Fe <sub>3</sub> O <sub>4</sub> @P(MMA-AA-DVB)	Emulsion	Water in water			98	Ali et al., 2015a)

1370  
1371  
1372  
1373  
1374  
1375  
1376  
1377  
1378  
1379  
1380  
1381  
1382  
1383  
1384  
1385  
1386  
1387



1389  
 1390 **Scheme 1.** Schematic illustration of magnetic solid-phase extraction process.  
 1391

1392  
 1393  
 1394  
 1395  
 1396

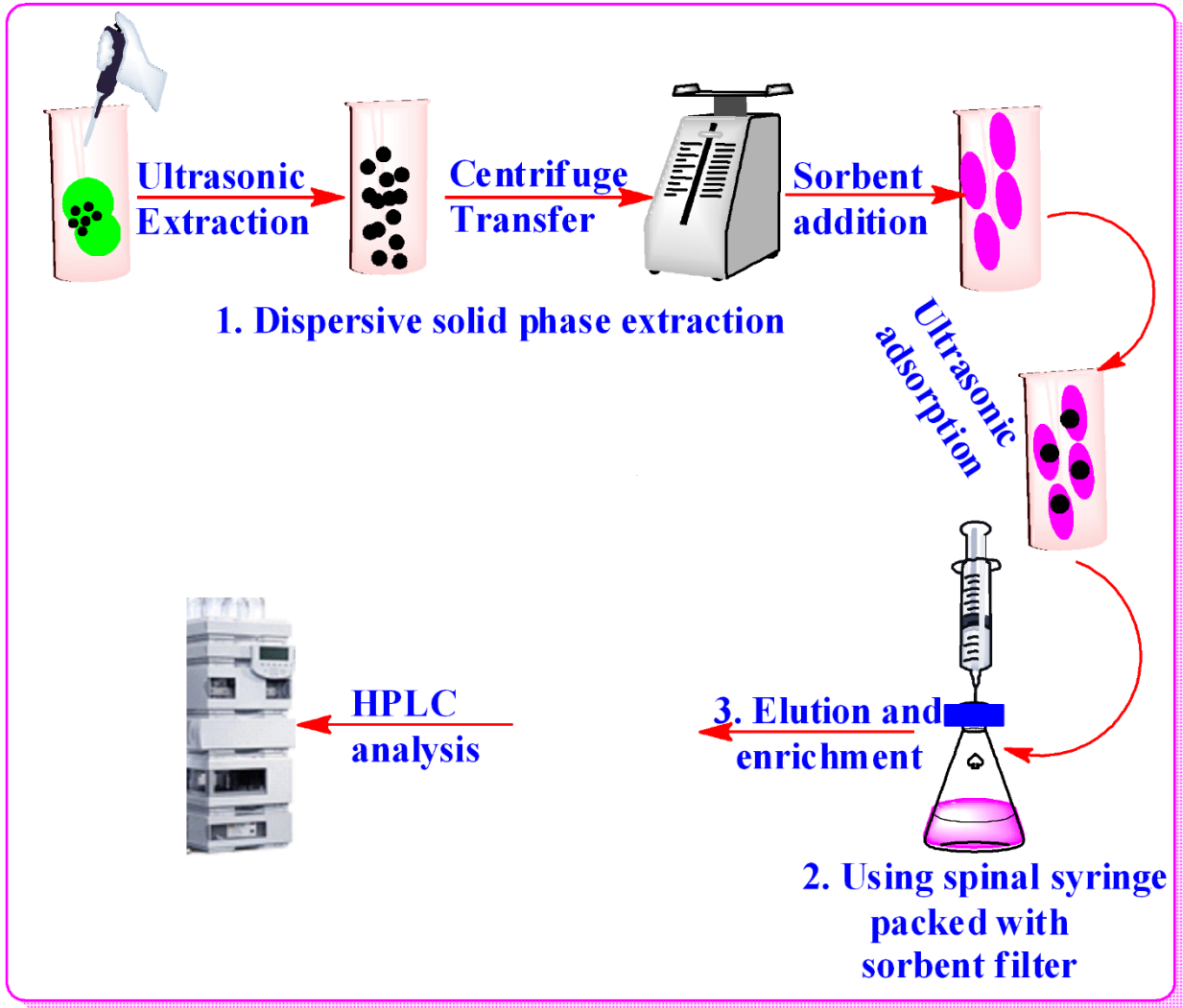
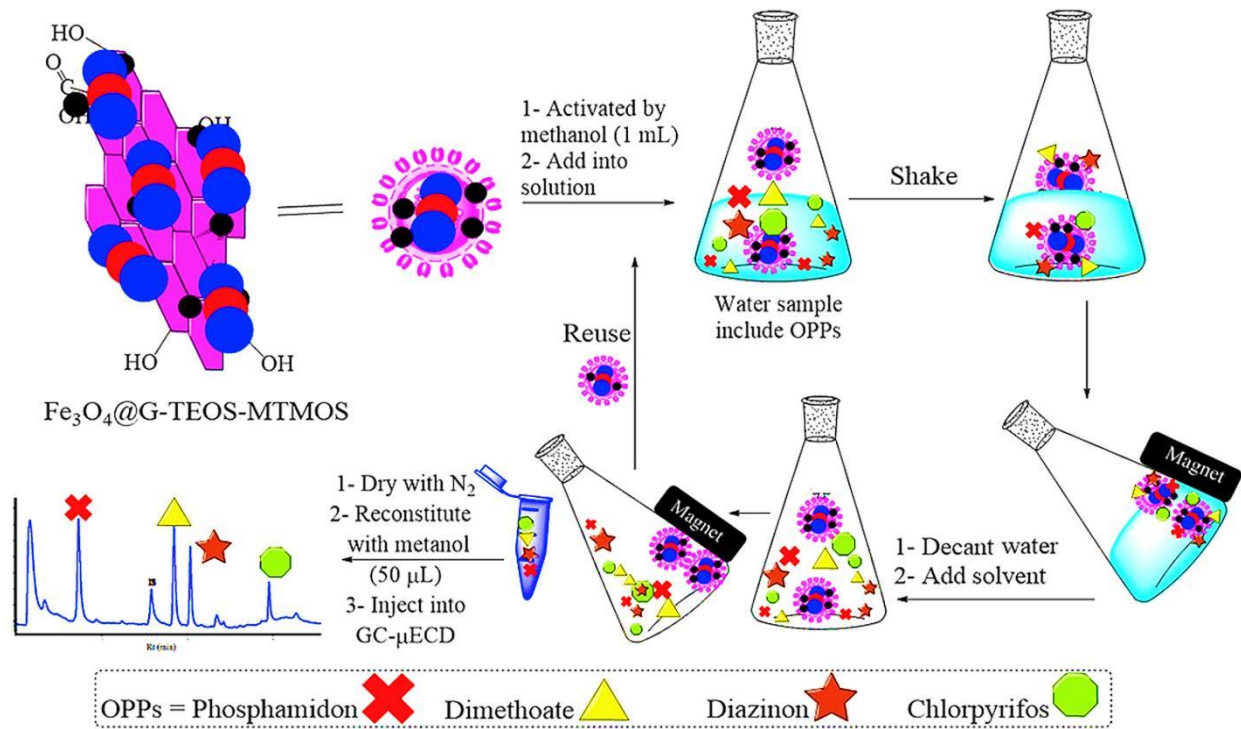


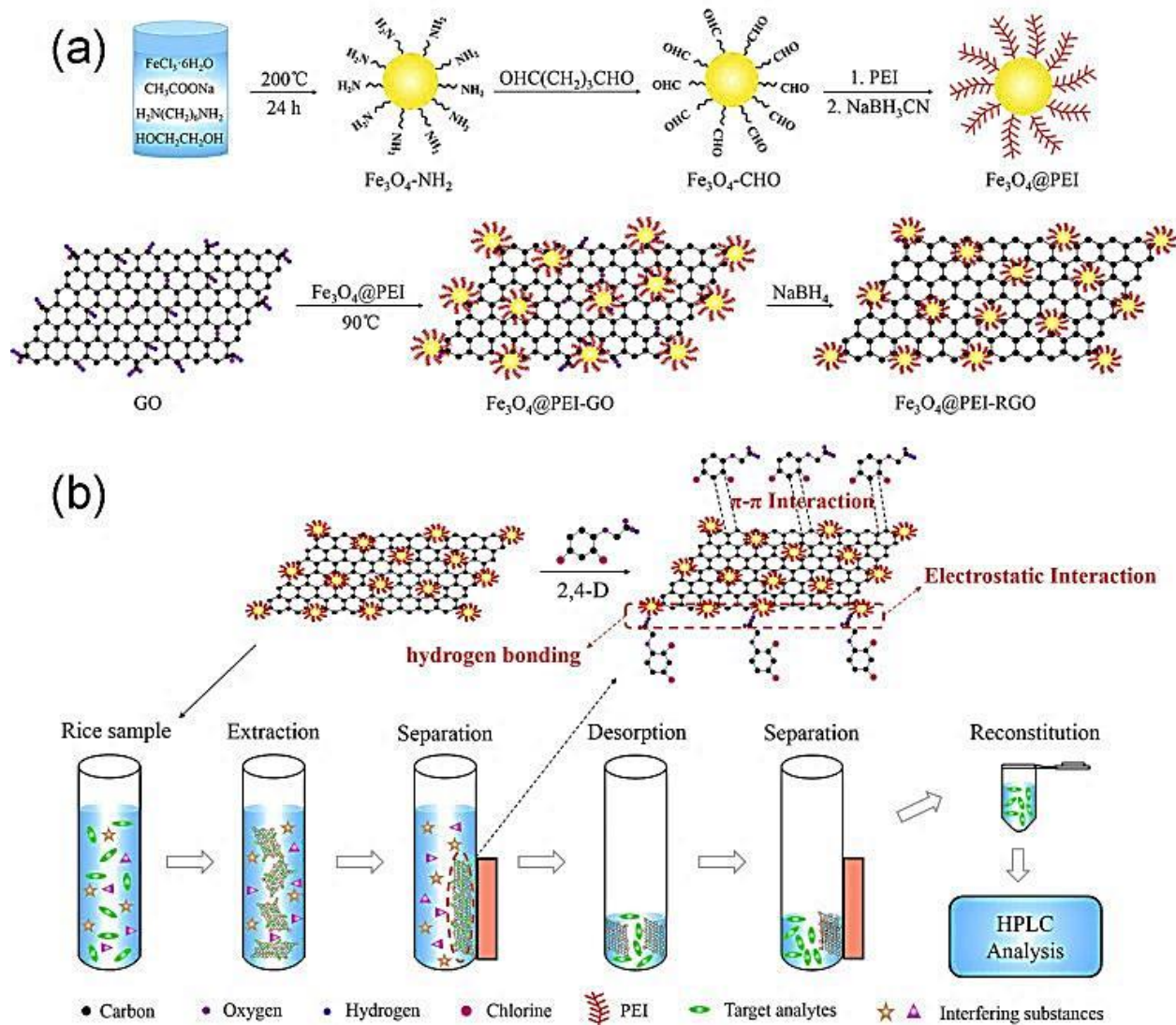
**Fig. 1** Schematic of the solid-phase extraction process.

1397  
 1398  
 1399  
 1400  
 1401  
 1402  
 1403  
 1404  
 1405  
 1406  
 1407  
 1408



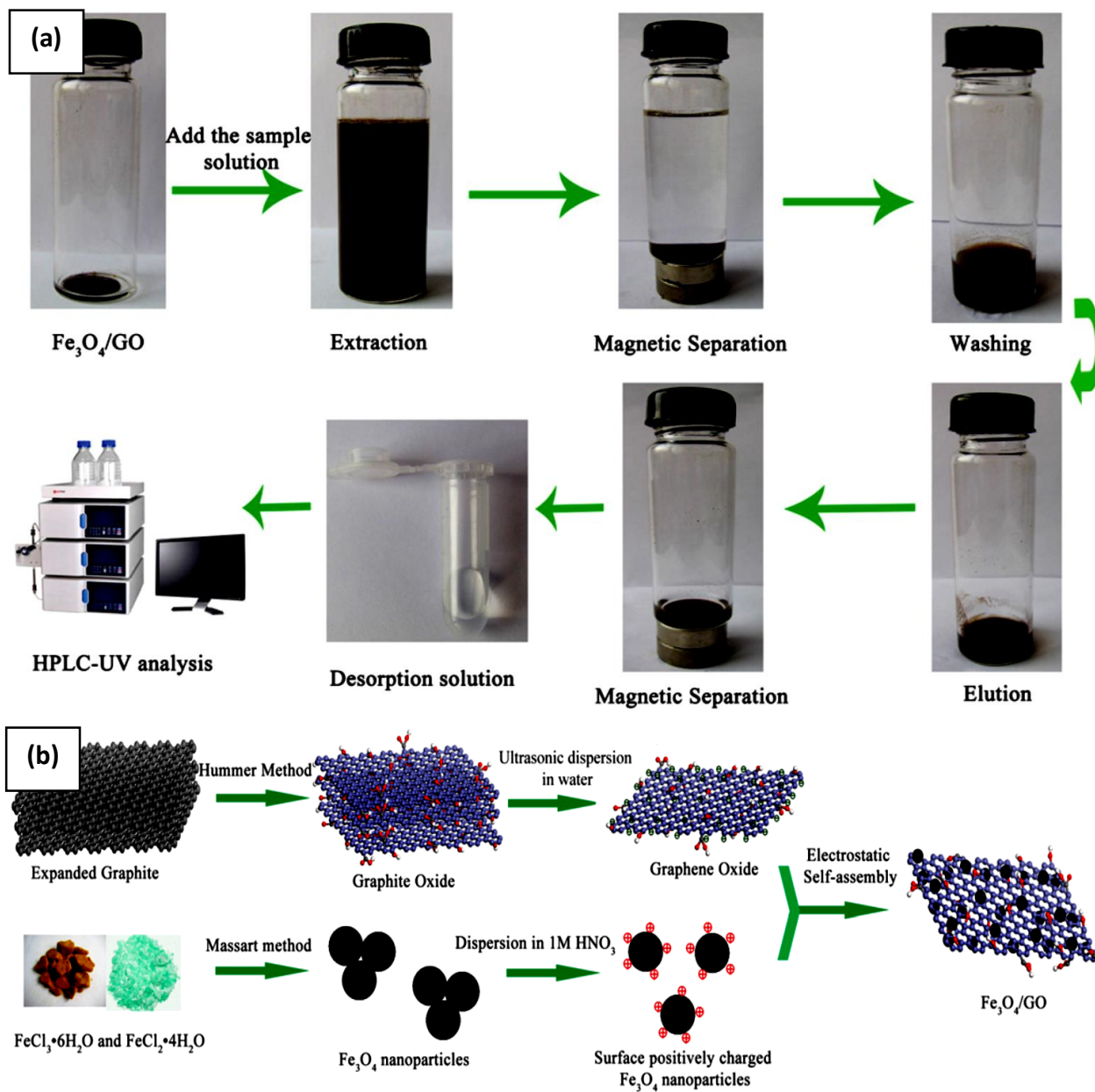
1409  
1410  
1411  
1412  
1413  
1414  
1415  
1416  
1417  
1418  
1419  
1420  
1421  
1422  
1423  
1424  
1425  
1426

**Fig. 2** Synthesis and MSPE applications of  $\text{Fe}_3\text{O}_4@\text{G-TEOS-MTMOS}$ . Reprinted from Nodeh et al. (2017) with permission from Elsevier. License Number: 5086230780822.



1427  
 1428 **Fig. 3** Schematic illustration for the synthesis of Fe<sub>3</sub>O<sub>4</sub>@PEI-RGO and their MSPE  
 1429 removal application. Reprinted from Li et al. (2017a) with permission from Elsevier.  
 1430 License Number: 5086250405992.

1431  
 1432  
 1433  
 1434  
 1435  
 1436  
 1437  
 1438



1439

1440

1441 **Fig. 4** (a) Experimental process for solid-phase extraction using  $\text{Fe}_3\text{O}_4/\text{GO}$ . (b) Schematic

1442 explanation of  $\text{Fe}_3\text{O}_4/\text{GO}$  nanocomposite fabrication. Reprinted from Han et al. (2012)

1443 with permission from Elsevier. License Number: 5086230981636.

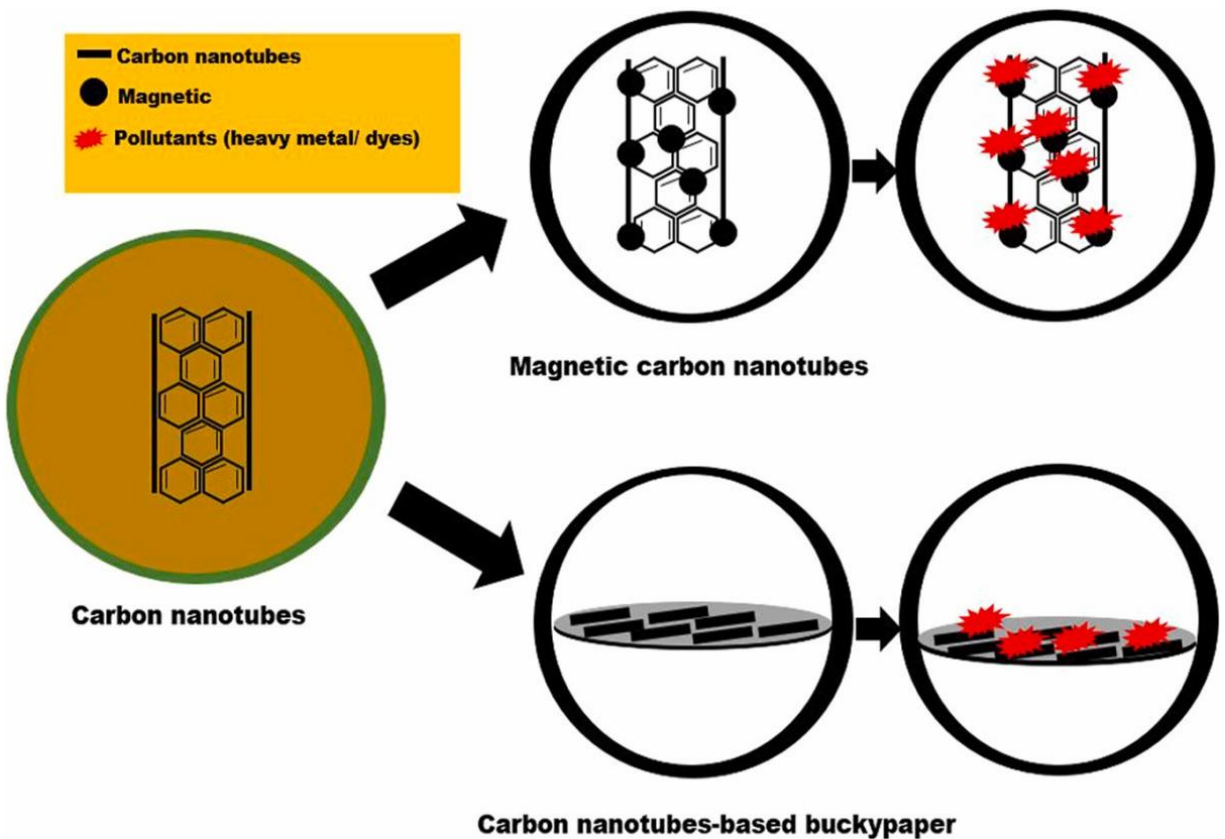
1444

1445

1446

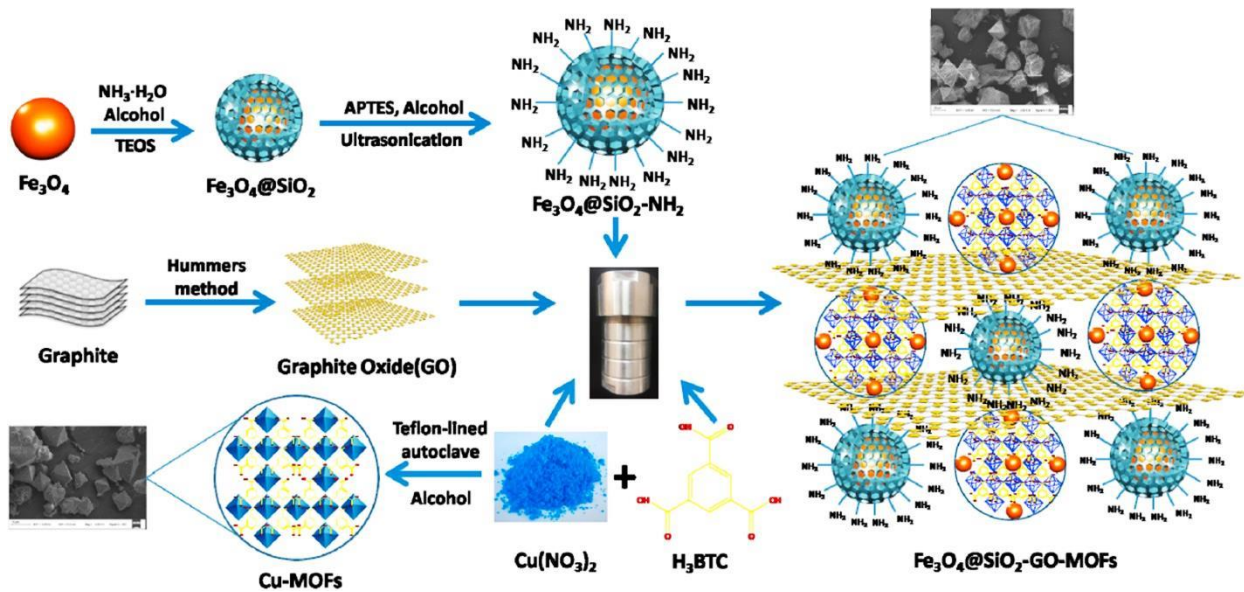
1447

1448



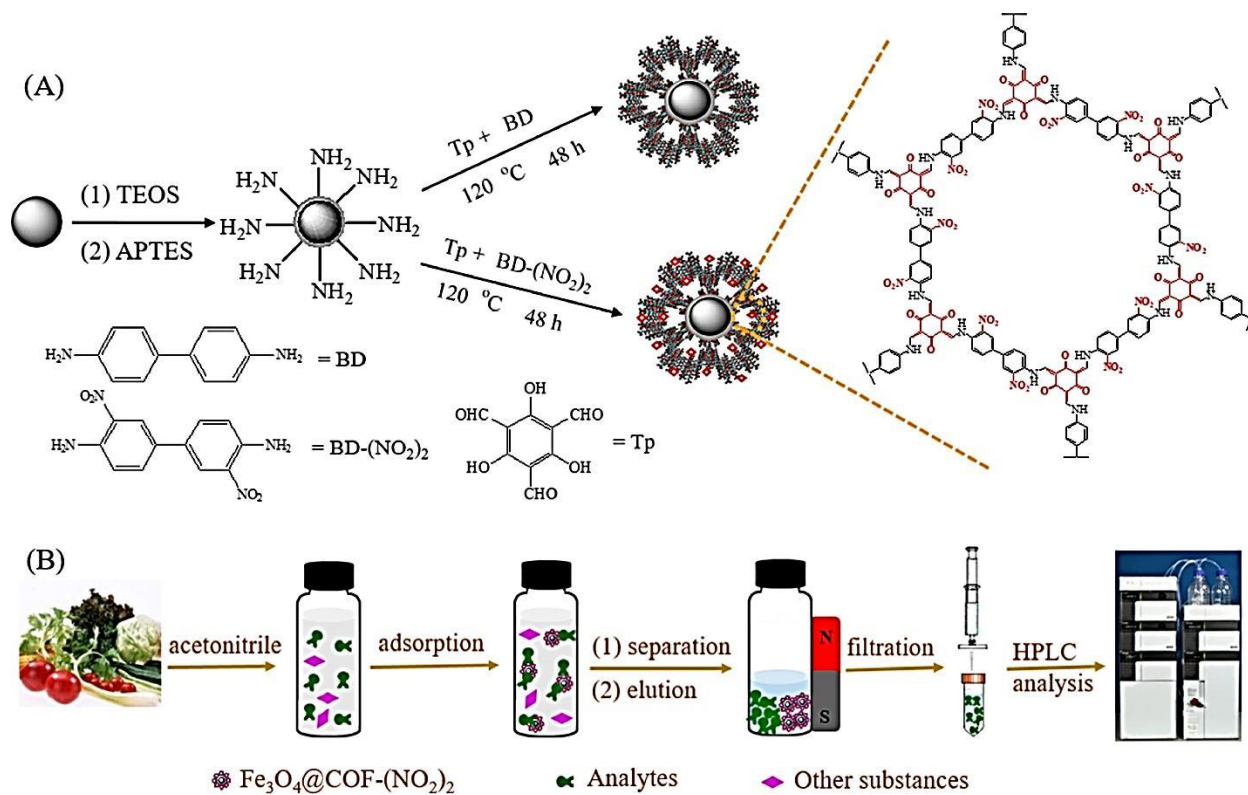
1449  
 1450  
 1451  
 1452  
 1453  
 1454  
 1455  
 1456  
 1457  
 1458  
 1459  
 1460  
 1461  
 1462  
 1463  
 1464  
 1465

**Fig. 5** Schematic illustration of MCNTs and carbon nanotube buckypaper for the effective removal of dyes and heavy metals. Reprinted from Khan et al. (2021e) with permission from Elsevier. License Number: 5086231420185.



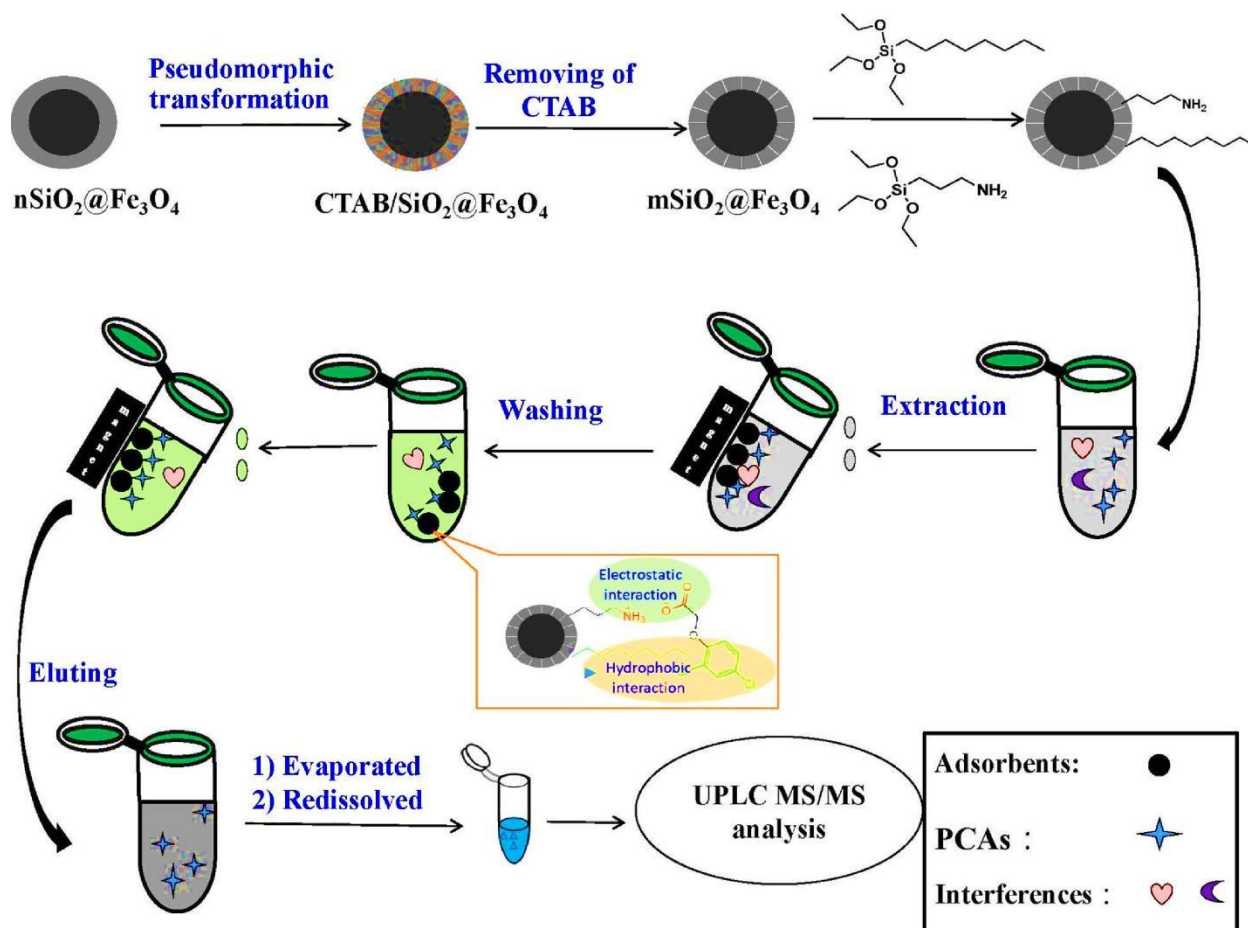
1466  
 1467 **Fig. 6** The layer-by-layer fabrication of Cu-MOFs and Fe<sub>3</sub>O<sub>4</sub>@SiO<sub>2</sub>-GO-MOFs magnetic  
 1468 nanocomposites. Reprinted from Wang et al. (2018b) with permission from Elsevier.  
 1469 License Number: 5086240269387

1470  
 1471  
 1472  
 1473  
 1474  
 1475  
 1476  
 1477  
 1478  
 1479  
 1480  
 1481  
 1482  
 1483  
 1484  
 1485  
 1486



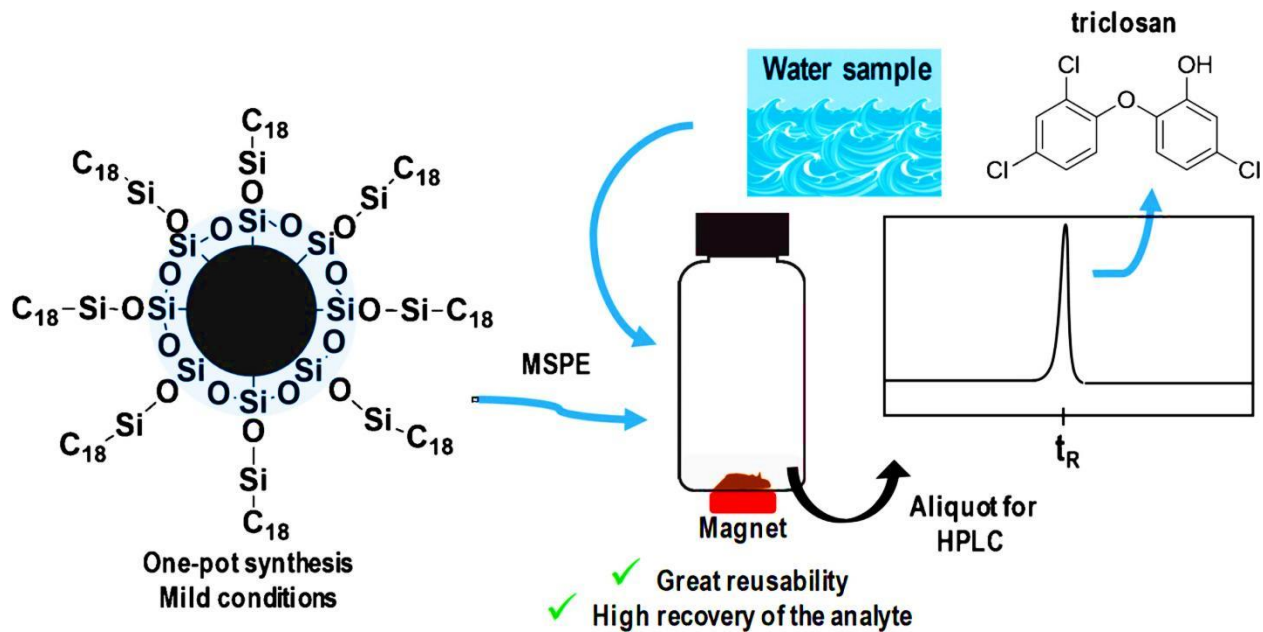
1487  
1488 **Fig. 7** (A) Schematic of the  $\text{Fe}_3\text{O}_4@ \text{COF}-(\text{NO}_2)_2$  microspheres synthesis. (B) MSPE  
1489 applications of  $\text{Fe}_3\text{O}_4@ \text{COF}-(\text{NO}_2)_2$  of different vegetable sample as sorbent. Reprinted  
1490 from Lu et al. (2020) with permission from Elsevier. License Number: 5086240628363.

1491  
1492  
1493  
1494  
1495  
1496  
1497  
1498  
1499  
1500  
1501  
1502  
1503



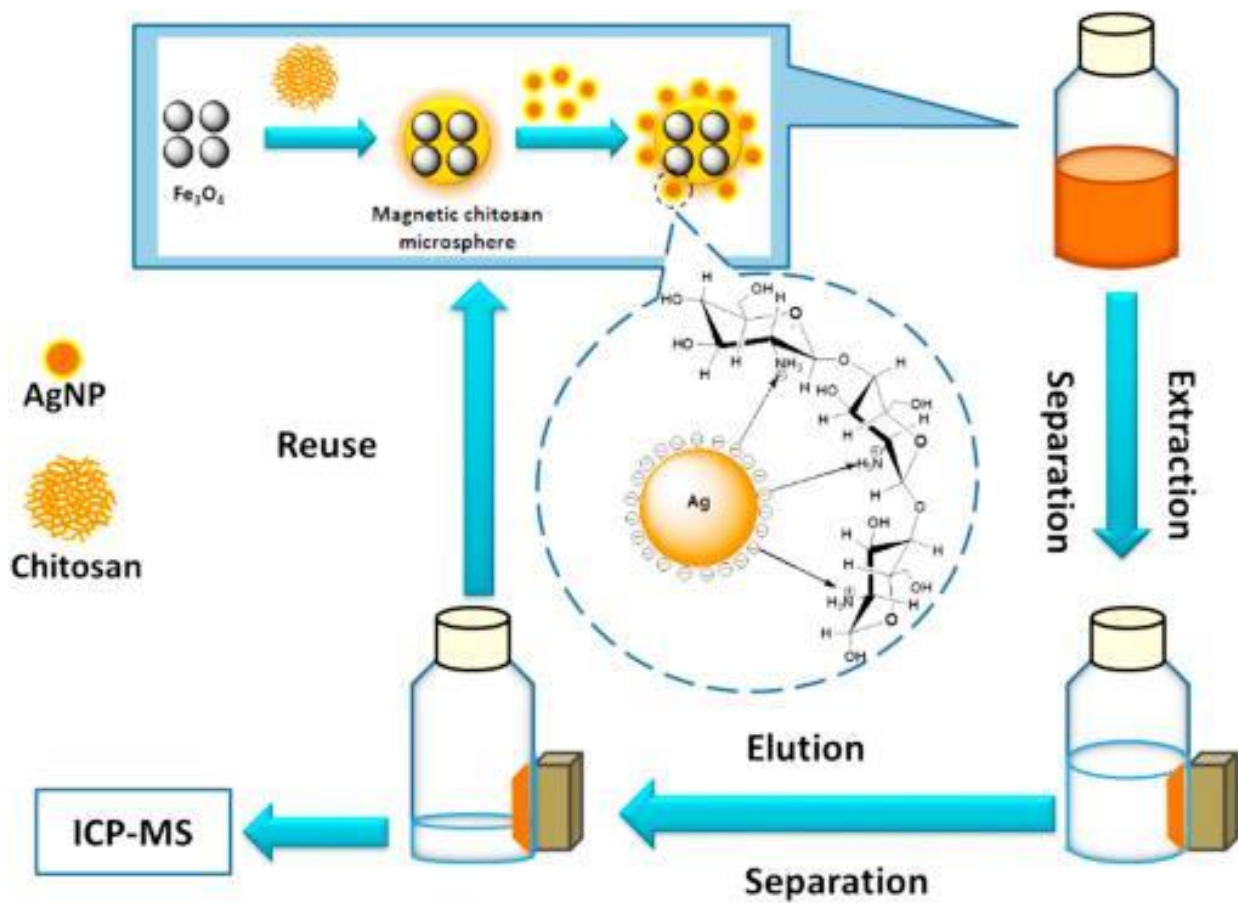
1504  
 1505  
 1506  
 1507  
 1508  
 1509  
 1510  
 1511  
 1512  
 1513  
 1514  
 1515  
 1516  
 1517  
 1518

**Fig. 8** Schematic illustration of mOAS synthesis and their application as an MSPE sorbent of PCAs from wastewater. Reprinted from Zhang et al. (2020) with permission from Elsevier. License Number: 5086250015810.



1519  
1520 **Fig. 9** One pot synthesis of  $\text{Fe}_2\text{O}_3@\text{SiO}_2\text{-C18}$  and their adsorption applications as MSPE  
1521 of triclosan. Reprinted from Caon et al. (2020) with permission from Elsevier. License  
1522 Number: 5086240852460.

1523  
1524  
1525  
1526  
1527  
1528  
1529  
1530  
1531  
1532  
1533  
1534  
1535  
1536  
1537  
1538



1539  
 1540 **Fig. 10** Schematic synthesis of magnetic chitosan microspheres sorbent and their  
 1541 application as MSPE sorbent of silver nanoparticles waste waters samples prior to the  
 1542 analysis of ICP-MS. Reprinted from Tolessa et al. (2017) with permission from Elsevier.  
 1543 License Number: 5086241063395.